Copy 407

532

[redacted] NASA TM X-583

NASA TM X-583

TECHNICAL MEMORANDUM

X-583

THE LATERAL AND DIRECTIONAL AERODYNAMIC CHARACTERISTICS OF A RE-ENTRY CONFIGURATION BASED ON A BLUNT 13° HALF CONE AT MACH NUMBERS TO 0.90

By George C. Kenyon

Ames Research Center
Moffett Field, Calif.

N67 11355 (ACCESSION NUMBER) ______ (THRU)

50 (PAGES) 1 (CODE)

TMX-583 (NASA CR OR TMX OR AD NUMBER) 01 (CATEGORY)

FACILITY FORM 602

NATIONAL AERONAUTICS AND SPACE ADMINISTRATION

WASHINGTON [redacted] November 1961

[redacted]

NATIONAL AERONAUTICS AND SPACE ADMINISTRATION

TECHNICAL MEMORANDUM X-583

THE LATERAL AND DIRECTIONAL AERODYNAMIC CHARACTERISTICS OF A RE-ENTRY CONFIGURATION BASED ON A BLUNT 13° HALF CONE AT MACH NUMBERS TO 0.90*

By George C. Kenyon

SUMMARY

A wind-tunnel investigation has been made to evaluate the subsonic aerodynamic characteristics of a lifting-body re-entry configuration based on a 13° half cone. The longitudinal characteristics of the basic configuration have been presented in NASA TM X-571. The present report presents the lateral and directional characteristics at Mach numbers from 0.25 to 0.90, including the effects of removing the canopy and the effects of adding dorsal and ventral fins. Since the latter changes in configuration were not included in the study of longitudinal characteristics presented in NASA TM X-571, some data are included in an appendix to this report showing the effects on longitudinal characteristics of removing the canopy and of adding a dorsal fin. The tests at a Mach number of 0.25 were conducted at a Reynolds number of 15 million based on body length; tests at Mach numbers from 0.60 to 0.90 were conducted at a Reynolds number of 5 million.

The test results indicate that the basic model was directionally unstable at small angles of sideslip for Mach numbers above 0.70. The addition of a dorsal fin completely eliminated this instability with only a small increase in positive dihedral effect. A ventral fin was ineffective. Side-mounted flaps and outboard elevons provided effective yaw and roll control. Removal of the canopy slightly improved the aerodynamic characteristics in both pitch and yaw.

INTRODUCTION

The Ames Research Center has conducted a research program on the characteristics of some re-entry configurations evolved from a blunt 13° half cone (refs. 1 to 3). As a result of this program a detailed

*Title, Unclassified

aerodynamic study has been made of a particular configuration consisting of a boattailed half-cone body, a canopy, vertical stabilizing surfaces, an upper surface trailing-edge flap, side-mounted yaw flaps, and outboard elevons. Reference 4 presents the longitudinal stability, performance, and control characteristics of this configuration at Mach numbers from 0.25 to 0.92 and reference 5 presents the supersonic longitudinal, lateral, and directional characteristics at Mach numbers to 5.0.

The present report presents the subsonic static lateral and directional aerodynamic characteristics of the study configuration in the Ames 12-Foot Pressure Wind Tunnel. Tests at a Mach number of 0.25 were conducted at a Reynolds number of 15 million based on model length and those at Mach numbers from 0.60 to 0.90 were conducted at a Reynolds number of 5 million. The effects of a dorsal fin and a ventral fin on the lateral and directional stability were determined. The effectiveness of the yaw flaps and elevons as yaw and roll controls were also evaluated.

The appendix to this report presents data, supplementing that given in reference 4, relative to the longitudinal characteristics of the study configuration with a dorsal fin and also with the canopy removed.

NOTATION

The results of the investigation are presented in the form of standard coefficients of forces and moments. These coefficients are referred to the body axes, with the exception of lift coefficient which is referred to the stability axis. The moment center was located at 55 percent of the length from the nose and 7 percent of the length below the cone axis. The coefficients and symbols used are defined as follows:

b body span at the base

C_L lift coefficient, $\frac{\text{lift}}{qS}$

C_l rolling-moment coefficient, $\frac{\text{rolling moment}}{qbS}$

C_m pitching-moment coefficient, $\frac{\text{pitching moment}}{q\bar{c}S}$

C_n yawing-moment coefficient, $\frac{\text{yawing moment}}{qbS}$

C_Y side-force coefficient, $\frac{\text{side force}}{qS}$

$\frac{L}{D}$ lift-drag ratio, $\frac{\text{lift}}{\text{drag}}$

l body length

M free-stream Mach number

q free-stream dynamic pressure

R Reynolds number, based on body length

S body plan-form area

α angle of attack, referenced to cone axis

β angle of sideslip

δ_e elevon deflection, positive with trailing edge down, measured from plane parallel to cone axis

δ_f trailing-edge flap deflection, positive trailing edge down, measured from tangent to upper surface at the base

δ_p pitch-flap deflection, positive with trailing edge down, measured from tangent to lower surface of the model

δ_y yaw-flap deflection, measured from the side of the model

Subscript

β partial derivative with respect to sideslip angle, evaluated at 0° sideslip angle

MODEL

The selection of geometric characteristics of the model was based on the results of the preliminary investigations reported in references 1 and 2 and is discussed in reference 4. Geometric properties of the model are given in figure 1 and photographs are presented in figure 2. The body shape was that of a half cone (with a 13° semiapex angle), blunted at the nose and boattailed at the rear, with the sides and bottom flattened in the region of the boattail. A canopy was fitted to the upper surface. The outboard elevons were mounted on the flat-surfaced vertical fins that extended above the body. The yaw flaps were mounted on the sides of the body and canted 15° to the cone axis. Dorsal and ventral fins (figs. 1(b)

and 2(b)) were also fitted to the basic model. The plan-form area of the control surfaces, in percent of body plan-form area, were as follows:

Each elevon	4.4 percent
Each yaw flap	2.6
Each vertical fin	8.7
Dorsal fin	15.3
Ventral fin	5.2

The model was equipped with two additional movable surfaces for longitudinal control. These consisted of a trailing-edge flap extending from the upper surface, and a pair of flaps (pitch flaps) mounted on the rear lower surface. The yaw flaps could be used as speed brakes when deflected simultaneously on each side of the body and were so considered in reference 4.

The model was constructed of wood fitted around a steel inner structure that incorporated a mounting for the six-component strain-gage balance. The whole assembly was supported on a 2.5-inch diameter sting. The model was painted with lacquer and hand rubbed with No. 400 sandpaper to a smooth finish.

TESTS

The lateral and directional characteristics of the model were investigated over a Mach number range of 0.25 to 0.90. Side force, rolling moment, and yawing moment were measured. Tests at a Mach number of 0.25 were conducted at a Reynolds number of 15 million based on body length (37 inches) and tests at Mach numbers of 0.60 to 0.90 were conducted at a Reynolds number of 5 million. Data were obtained for sideslip angles from -8° to $+18^\circ$ with the model fixed at angles of attack of 0°, 6°, and 12° at a Mach number of 0.25, and at an angle of attack of 6° at Mach numbers from 0.60 to 0.90. Tests were made through the Mach number range at angles of attack from -8° to $+18^\circ$ with the model fixed at sideslip angles of 0° and -6°.

Variations in the basic test configuration included the addition of a dorsal fin, the addition of a ventral fin, removal of the vertical fins, and removal of the canopy. Yaw control effectiveness was studied by deflecting the left yaw flap on the basic configuration. Elevon effectiveness with respect to roll control was studied by deflecting the elevons asymmetrically on the basic configuration with yaw flaps retracted. In general, the longitudinal controls, including the elevons, lower surface pitch flaps, and the trailing-edge flap, were maintained at angles that resulted in reasonable trim conditions. The trailing-edge flap is considered only as a low-speed trimming device; hence, it was removed for tests at Mach number 0.60 to 0.90.

Since the investigation of reference 4 did not include the longitudinal characteristics of the study configuration with dorsal fin or with canopy removed, these characteristics were evaluated and the data are presented in the appendix.

CORRECTIONS TO DATA

The method of reference 6 was used to correct the data for constriction effects due to the tunnel walls. The corrections to Mach number and dynamic pressure were as follows:

Corrected Mach No.	Uncorrected Mach No.	$\frac{q_{corrected}}{q_{uncorrected}}$
0.25	0.25	1.003
.60	.598	1.004
.70	.698	1.005
.80	.795	1.008
.85	.843	1.010
.90	.888	1.015

RESULTS AND DISCUSSION

Low Speed Tests (M = 0.25)

The low-speed lateral and directional characteristics of the basic model are presented in figure 3 as functions of sideslip angle. These data were obtained with various amounts of longitudinal control deflection at angles of attack of 0°, 6°, and 12°. These angles and control deflections represent longitudinal trim conditions at lift coefficients of approximately 0.2, 0.4, and 0.6, respectively (see ref. 4). The moment center was located at 55 percent of the length from the nose and 7 percent of the length below the cone axis. The data show that the model was directionally stable to a sideslip angle of at least 10° and had a large positive dihedral effect. At sideslip angles beyond 10°, the yawing moment exhibited an unstable trend at the higher angles of attack. Figure 4 presents the lateral and directional characteristics of the model as functions of angle of attack for fixed sideslip angles of 0° and -6°. These data show that, for a sideslip angle of -6°, the forces and moments were relatively insensitive to attitude change up to an angle of attack of about 15°.

Figure 5 shows the effects of adding the dorsal fin to the basic model. Also shown are data for the model without dorsal or vertical fins. The marked increase in directional stability due to the dorsal fin is obvious, but it is interesting to note that the addition of this large vertical surface above the model did not increase the rolling moment due to sideslip as might have been expected. It can also be seen from figure 5 that with the vertical fins removed the model was directionally unstable with the chosen moment center.

The effects of removing the canopy from the basic model are shown in figure 6. Removing the canopy about doubled the directional stability at sideslip angles of 6° or less but produced a sudden loss in directional stability at higher sideslip angles. Although the model was not tested with the dorsal fin installed and the canopy removed, it seems likely that this instability would be eliminated by addition of the dorsal fin.

Figure 7 presents the lateral- and directional-stability derivatives as functions of angle of attack. The derivatives were evaluated at 0° sideslip angle from the data of figures 3, 5, and 6.

The effects of deflecting the left yaw flap are shown in figures 8 and 9. These data show that the effectiveness of the yaw flap remained constant with increasing angle of sideslip (fig. 8) but decreased sharply with increasing angle of attack (fig. 9(a)). Elevon and yaw-flap interference effects were small for a yaw-flap deflection of 30° but were large for a 60° deflection.

The effects of asymmetric elevon deflection are presented in figure 10. The elevons provided roll control throughout the angle-of-attack range with little effect on the yawing moment.

High-Speed Tests (M = 0.60 to 0.90)

The high-speed tests were conducted at a Reynolds number of 5 million with the trailing-edge flap removed and with the pitch flaps extended 30°, representing a typical configuration for longitudinal trim in this speed range (see ref. 4).

The lateral and directional characteristics of the model are presented in figure 11 as functions of sideslip angle and in figure 12 as functions of angle of attack. The data show that the model with the dorsal fin was directionally stable and had a large positive dihedral effect. The force and moment curves were nearly linear. Without the dorsal fin, the model was unstable directionally at the higher Mach numbers and, at a Mach number of 0.90, the model exhibited a negative dihedral effect. The ventral fin

proved ineffective in either reducing the rolling moment due to sideslip or providing directional stability, possibly the result of interference between the deflected pitch flaps and the ventral fin.

The characteristics of the basic model without canopy are presented in figure 13. The removal of the canopy resulted in a marked increase in directional stability at small angles of sideslip at Mach numbers of 0.80 and above, but directional instabilities still occurred at angles of sideslip beyond about 3°. The effects of Mach number on the lateral and directional stability derivatives are shown in figure 14.

The effects of deflecting the left yaw flap on the lateral and directional characteristics are shown in figure 15. It can be seen that the yaw-flap effectiveness was relatively insensitive to increasing Mach number but decreased rapidly with increasing angle of attack, as was the case at a Mach number of 0.25.

A 4 8 8

The lateral and directional characteristics of the model with the elevons deflected asymmetrically as roll controls are presented in figure 16. In contrast to the results at low speed, these data show considerable cross-coupling; that is, deflection of the roll controls produced a yawing moment. Roll control reversal is also indicated for the higher angles of attack.

CONCLUSIONS

A wind-tunnel investigation has been conducted at subsonic Mach numbers varying from 0.25 to 0.90 to measure the aerodynamic characteristics of a lifting-body re-entry configuration, based on a 13° half cone. This report presents the lateral and directional characteristics of the configuration and shows the following:

1. The basic re-entry configuration was directionally stable at Mach numbers up to 0.70, but at higher Mach numbers it was directionally unstable for small angles of sideslip.

2. The addition of a dorsal fin provided excellent directional stability characteristics at all test Mach numbers, with only small increase in positive dihedral effect. A ventral fin was ineffective.

3. Removal of the canopy slightly improved the aerodynamic characteristics in pitch and in yaw to sideslip angles of 6° but did not eliminate the need for a dorsal fin to provide directional stability at higher sideslip angles.

4. Side-mounted flaps and outboard elevons provided effective yaw and roll controls.

Ames Research Center
National Aeronautics and Space Administration
Moffett Field, Calif., Aug. 25, 1961

APPENDIX

LONGITUDINAL CHARACTERISTICS OF THE MODEL

Reference 4 detailed the longitudinal aerodynamic characteristics of the study configuration. Subsequent to the publication of reference 4, two additional modifications to the model were investigated; namely, the model equipped with the dorsal fin and the model without the canopy. The lateral and directional characteristics of the model with these modifications have been presented in the body of this report. This appendix presents the longitudinal aerodynamic characteristics of the model with these two modifications.

Basic Model With Dorsal Fin

Figure 17 shows the longitudinal characteristics of the model equipped with the dorsal fin at a Mach number of 0.25 and a Reynolds number of 15 million, and figure 18 presents the characteristics of the model at Mach numbers from 0.60 to 0.90 at a Reynolds number of 5 million.

Basic Model Without Canopy

The longitudinal characteristics of the model without the canopy are shown in figure 19 for a Mach number of 0.25 and a Reynolds number of 15 million. Figure 20 shows the characteristics obtained at Mach numbers of 0.60 to 0.90 at a Reynolds number of 5 million.

REFERENCES

1. Kenyon, George C., and Edwards, George G.: A Preliminary Investigation of Modified Blunt 13° Half-Cone Re-entry Configurations at Subsonic Speeds. NASA TM X-501, 1961

2. Rakich, John V.: Supersonic Aerodynamic Performance and Static-Stability Characteristics of Two Blunt-Nosed Modified 13° Half-Cone Configurations. NASA TM X-375, 1960.

3. Dennis, David H., and Edwards, George G.: The Aerodynamic Characteristics of Some Lifting Bodies. NASA TM X-376, 1960.

4. Kenyon, George C., and Sutton, Fred B.: The Longitudinal Aerodynamic Characteristics of a Re-entry Configuration Based on a Blunt 13° Half Cone at Mach Numbers to 0.92. NASA TM X-571, 1961.

5. Rakich, John V.: Aerodynamic Performance and Static Stability of a Blunt-Nosed Boattailed 13° Half-Cone at Mach Numbers of 0.60 to 5.0. NASA TM X-570, 1961.

6. Herriot, John G.: Blockage Corrections for Three-Dimensional-Flow Closed Throat Wind Tunnels With Consideration of the Effect of Compressibility. NACA Rep. 995, 1950. (Supersedes NACA RM A7B28)

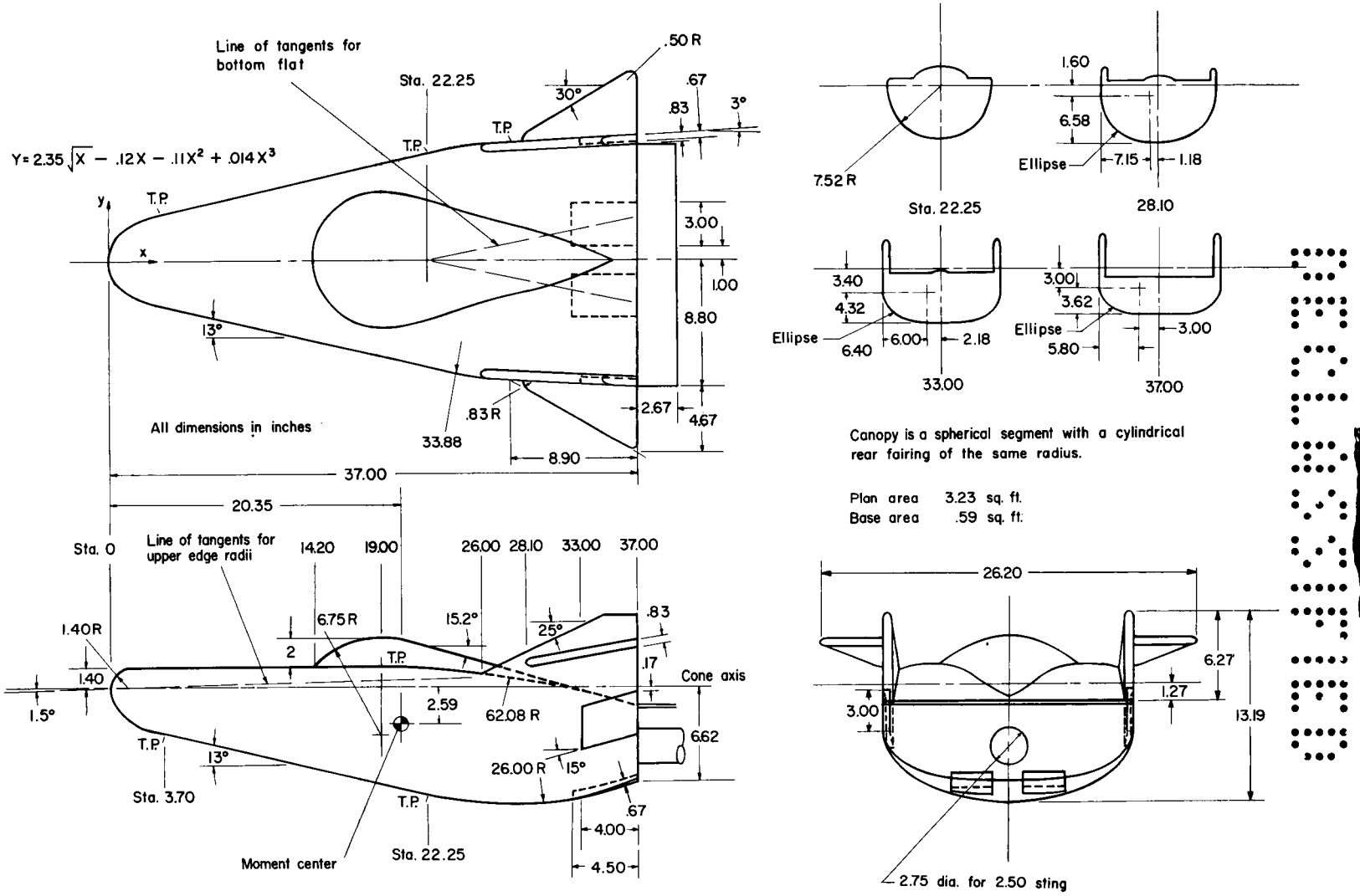

(a) General arrangement of the basic model.

Figure 1.- Geometry of the model.

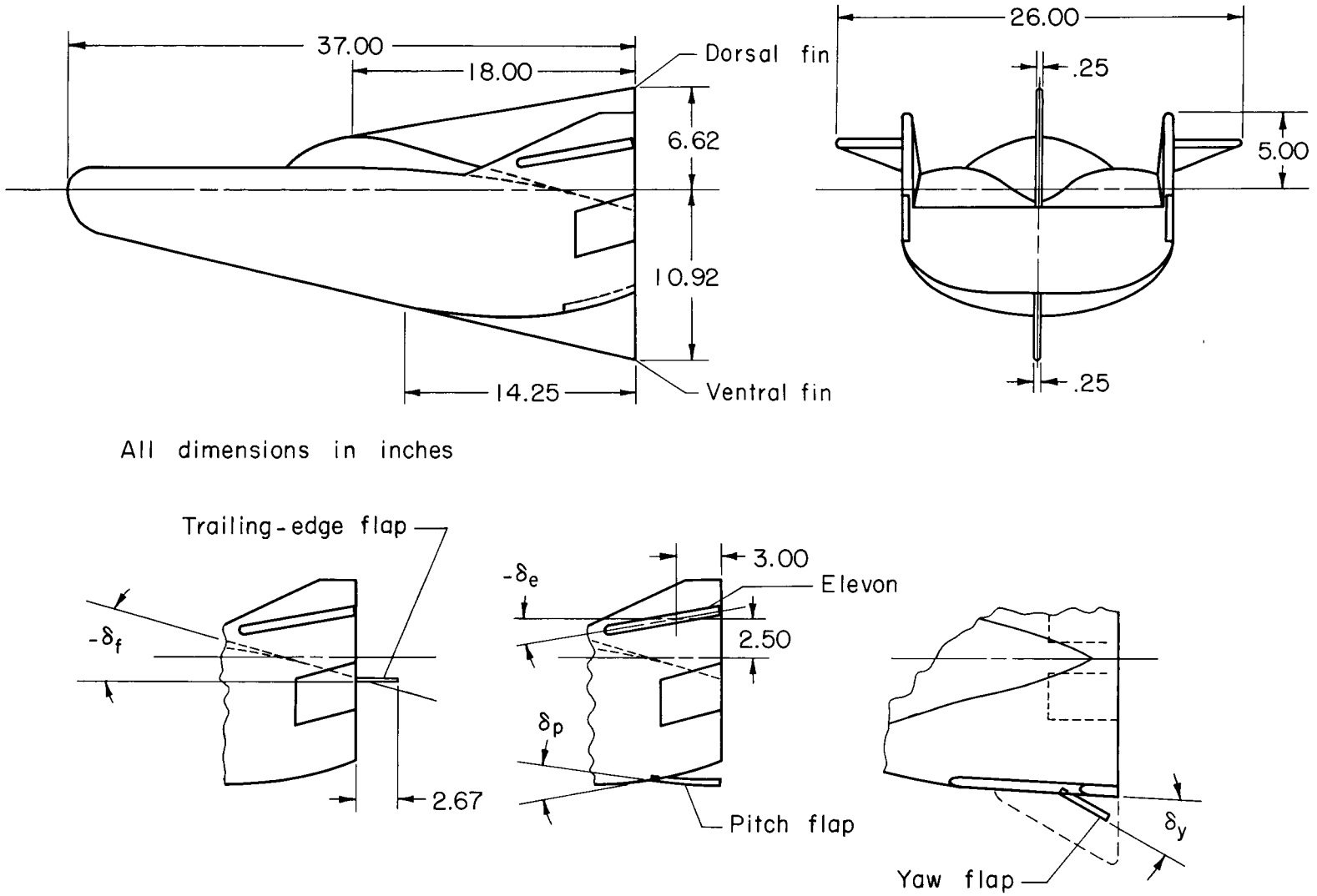

(b) Model details.

Figure 1.- Concluded.

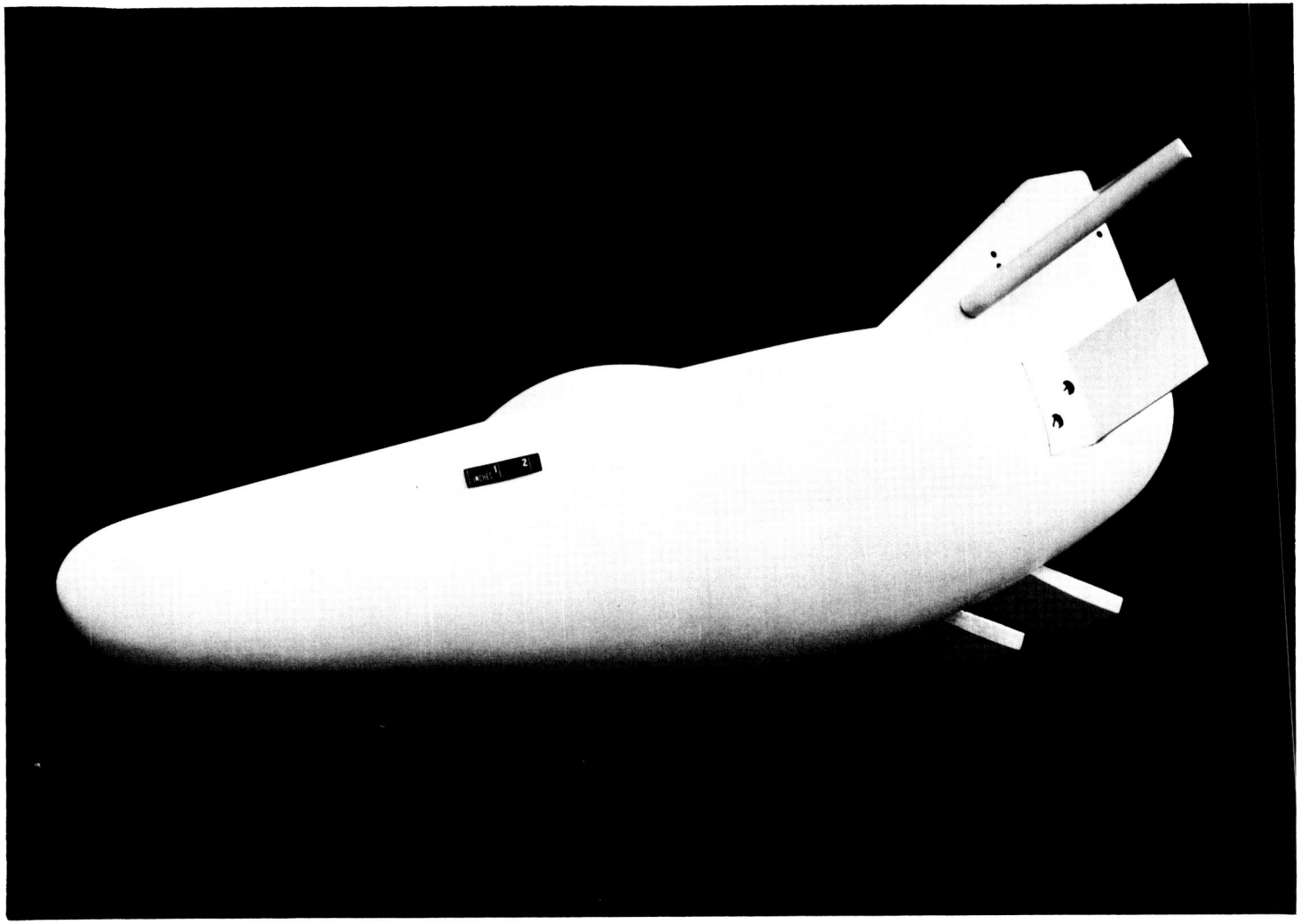

(a) The basic model with elevon, yaw flap, and pitch flaps deflected. A-26159

Figure 2.- Photographs of the model.

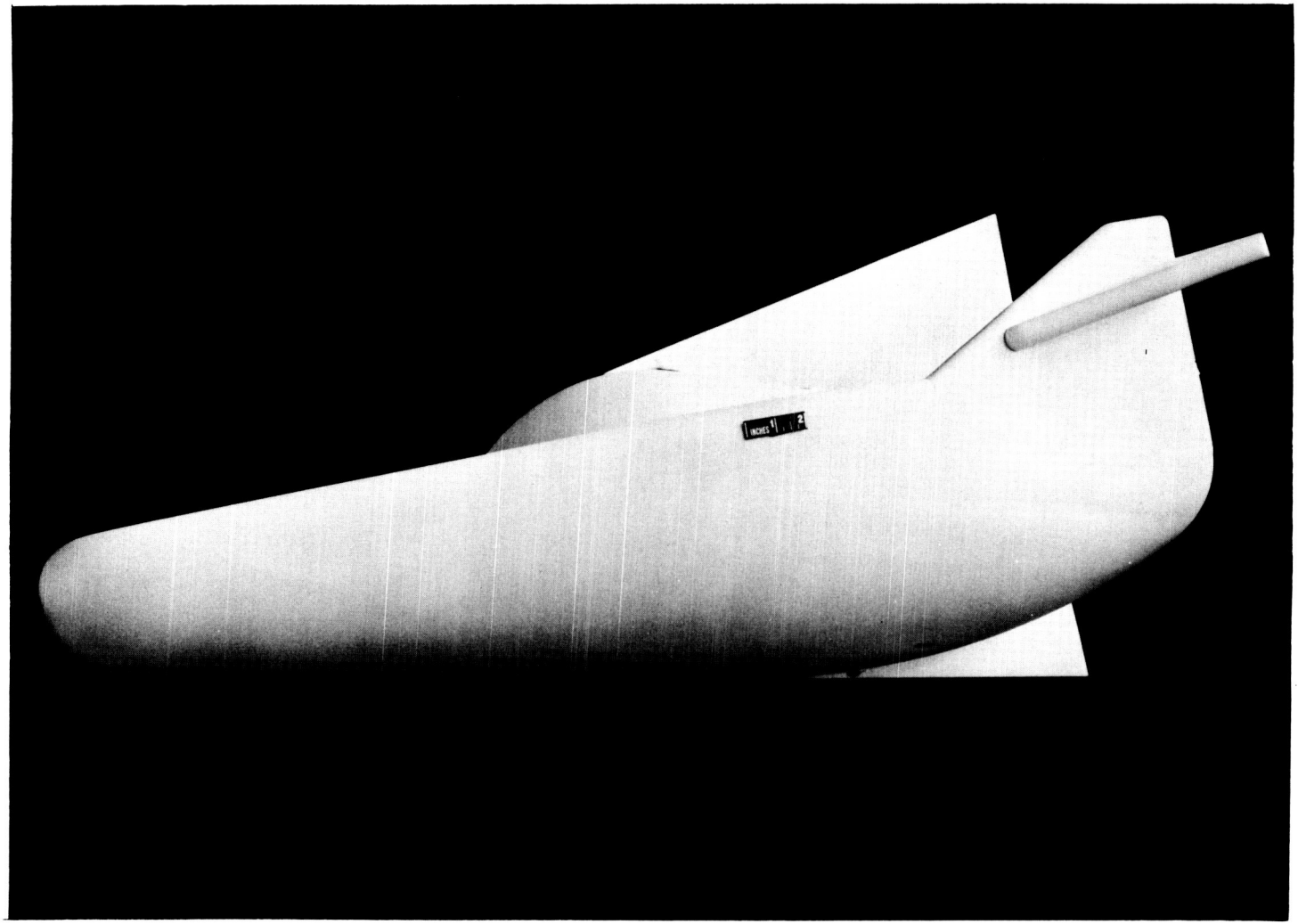

A-27095

(b) The basic model with the dorsal fin and the ventral fin.

Figure 2.- Concluded.

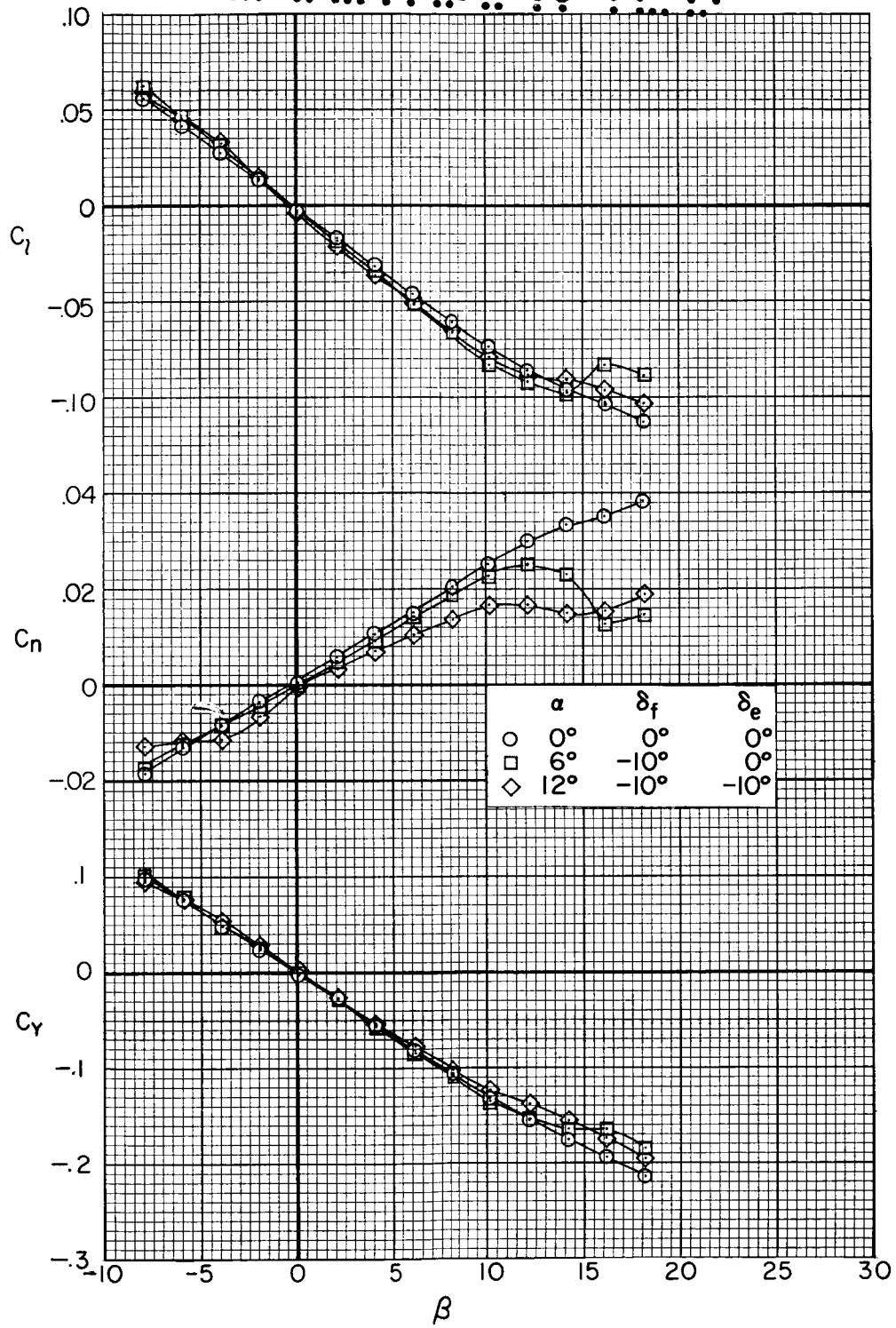

Figure 3.- The lateral and directional characteristics of the basic model at three angles of attack; R = 15X10^6, M = 0.25, $\delta_p = 0^\circ$.

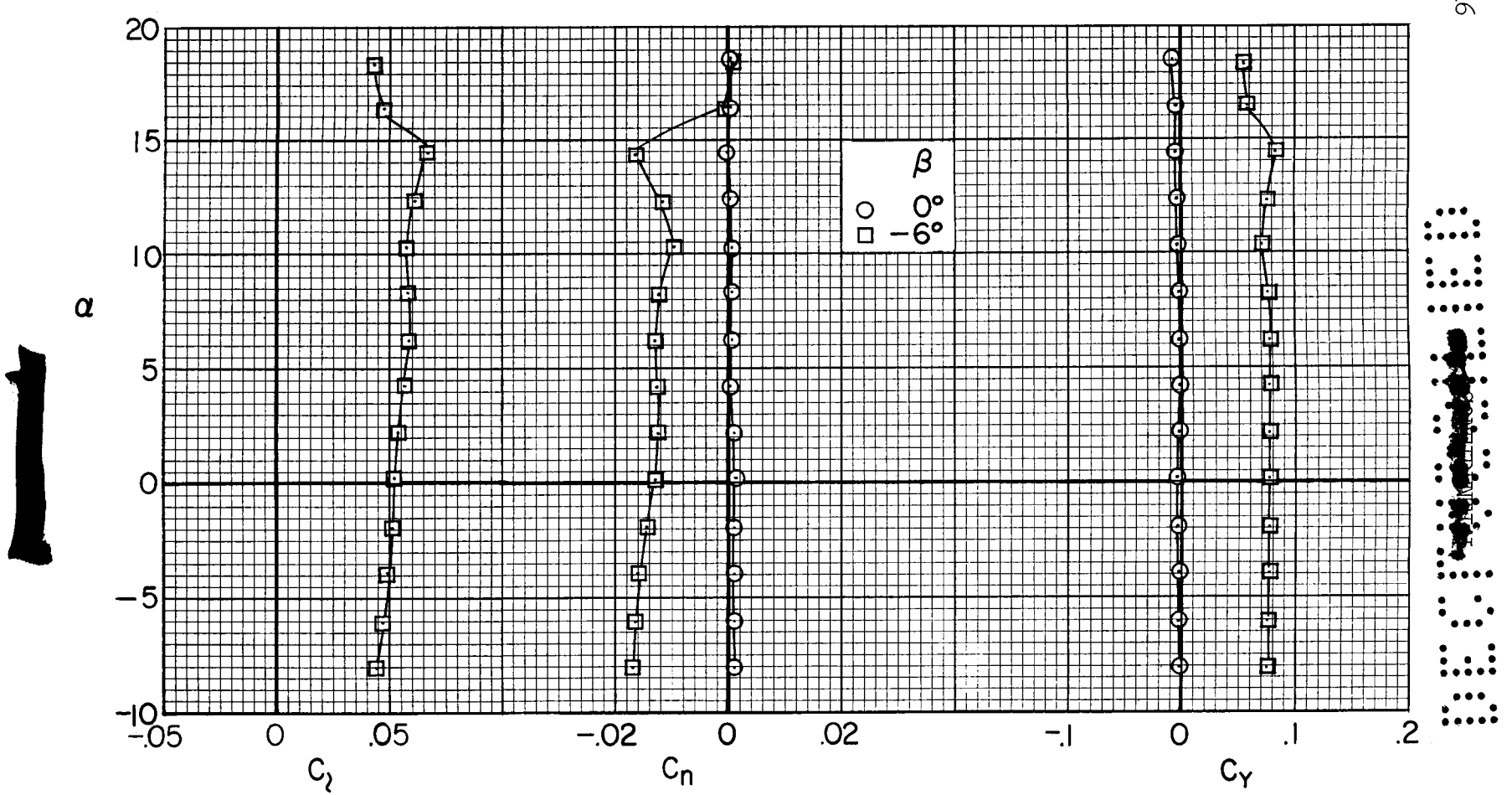

Figure 4.- The variation with angle of attack of the lateral and directional characteristics of the basic model; R = 15X10^6, M = 0.25, δ_e = -10°, δ_f = -10°, δ_p = 0°.

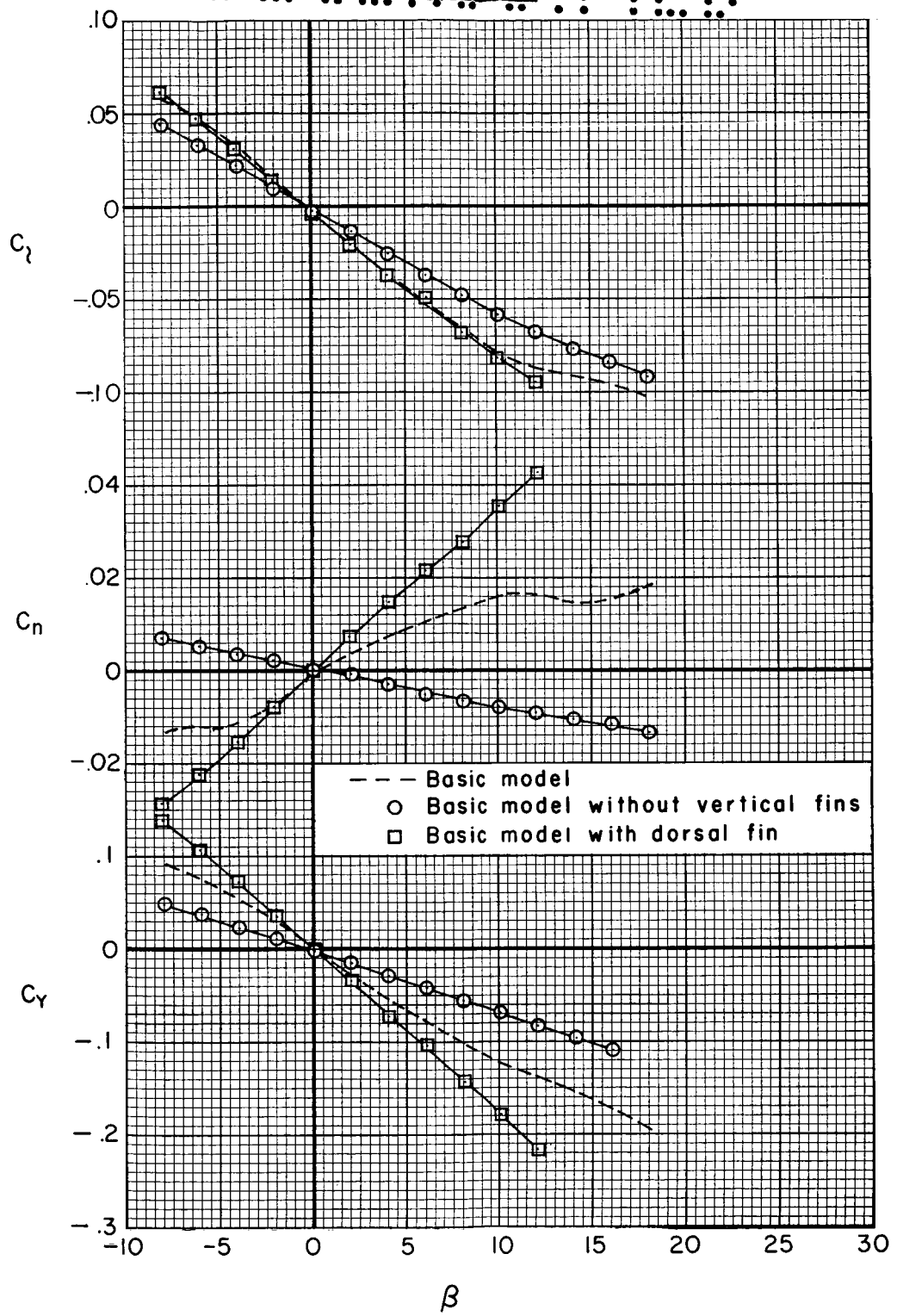

Figure 5.- The effects of the dorsal and vertical fins on the lateral and directional characteristics of the model; $\alpha = 12^{\circ}$, $R = 15 \times 10^{6}$, $M = 0.25$, $\delta_e = -10^{\circ}$, $\delta_f = -10^{\circ}$, $\delta_p = 0^{\circ}$.

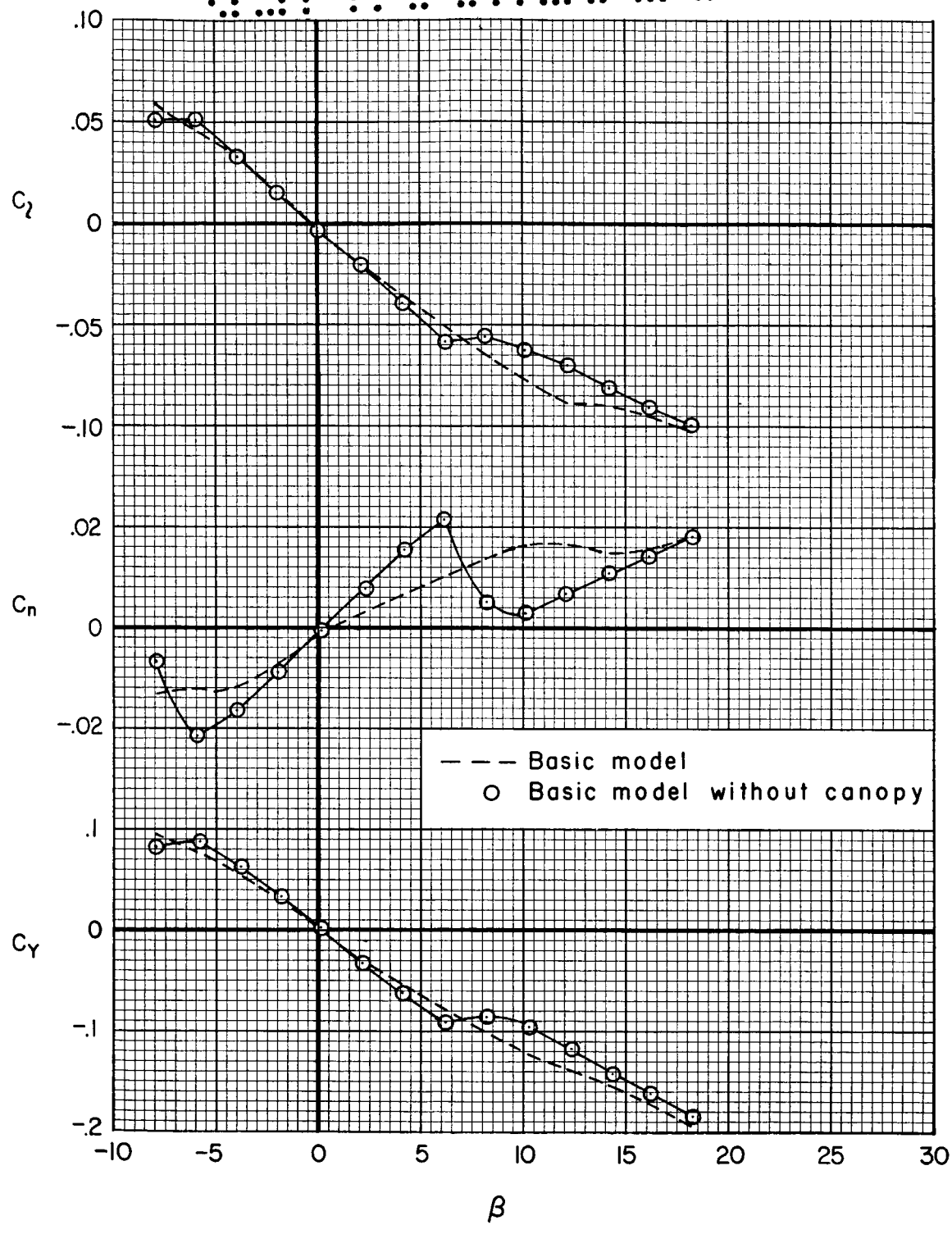

Figure 6.- The effects of removing the canopy on the lateral and directional characteristics of the basic model; $\alpha = 12^{\circ}$, $R = 15 \times 10^{6}$, $M = 0.25$, $\delta_e = -10^{\circ}$, $\delta_f = -10^{\circ}$, $\delta_p = 0^{\circ}$.

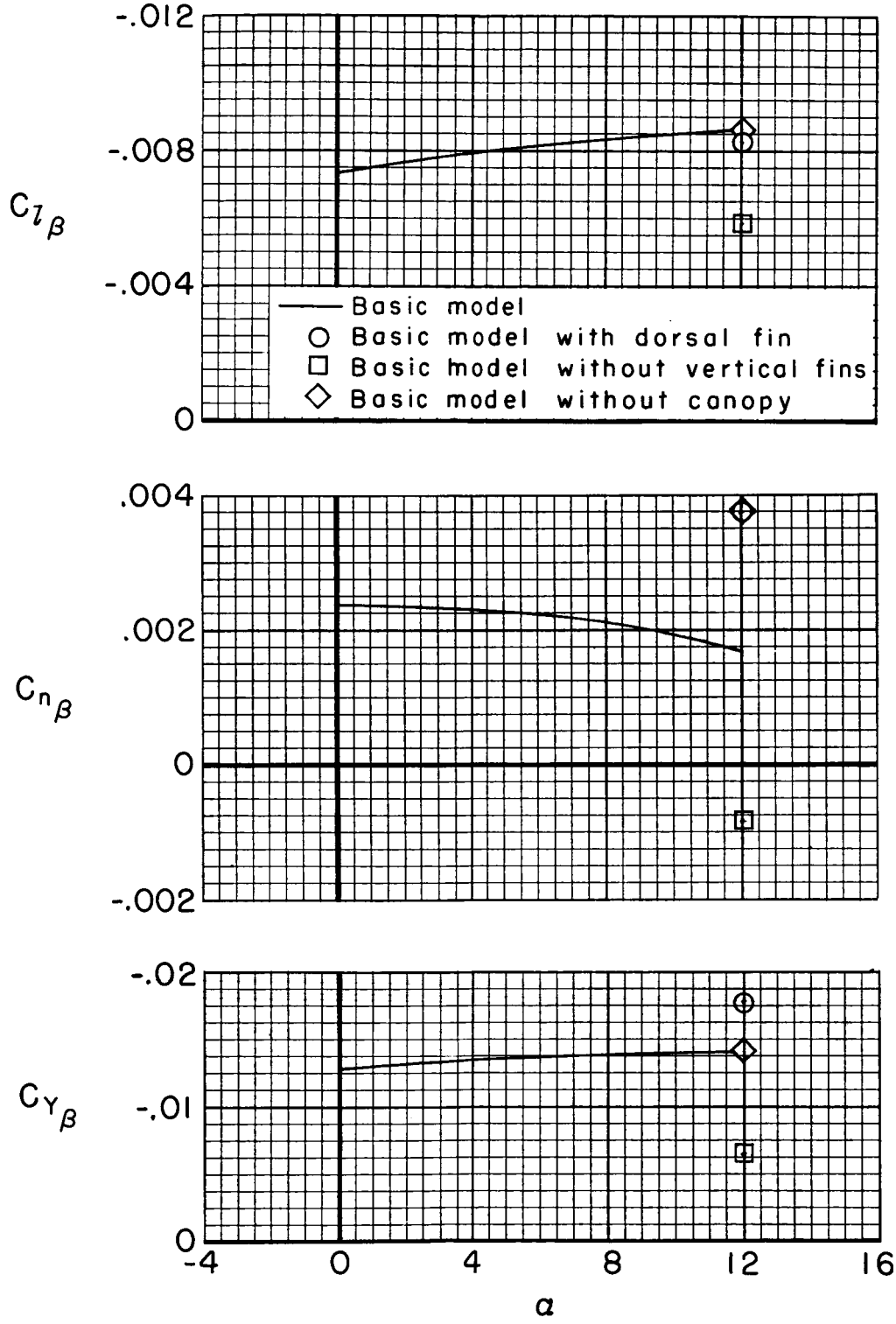

Figure 7.- The lateral and directional stability derivatives of the model evaluated at 0° sideslip angle; R = 15×10⁶, M = 0.25.

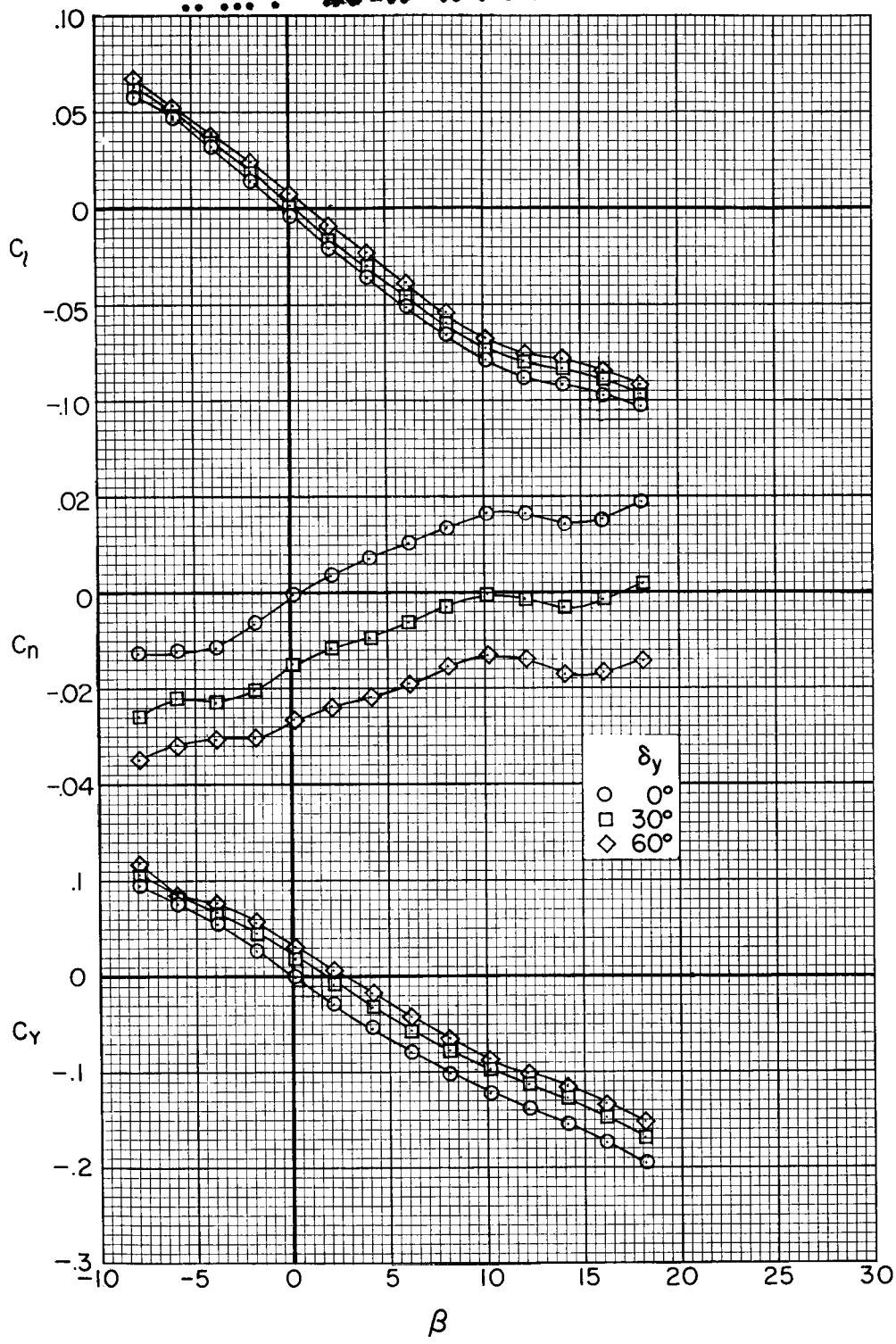

Figure 8.- The effects of deflecting the left yaw-flap on the lateral and directional characteristics of the basic model, for a range of sideslip angles; $\alpha = 12^{\circ}$, $R = 15 \times 10^{6}$, $M = 0.25$, $\delta_e = -10^{\circ}$, $\delta_f = -10^{\circ}$, $\delta_p = 0^{\circ}$.

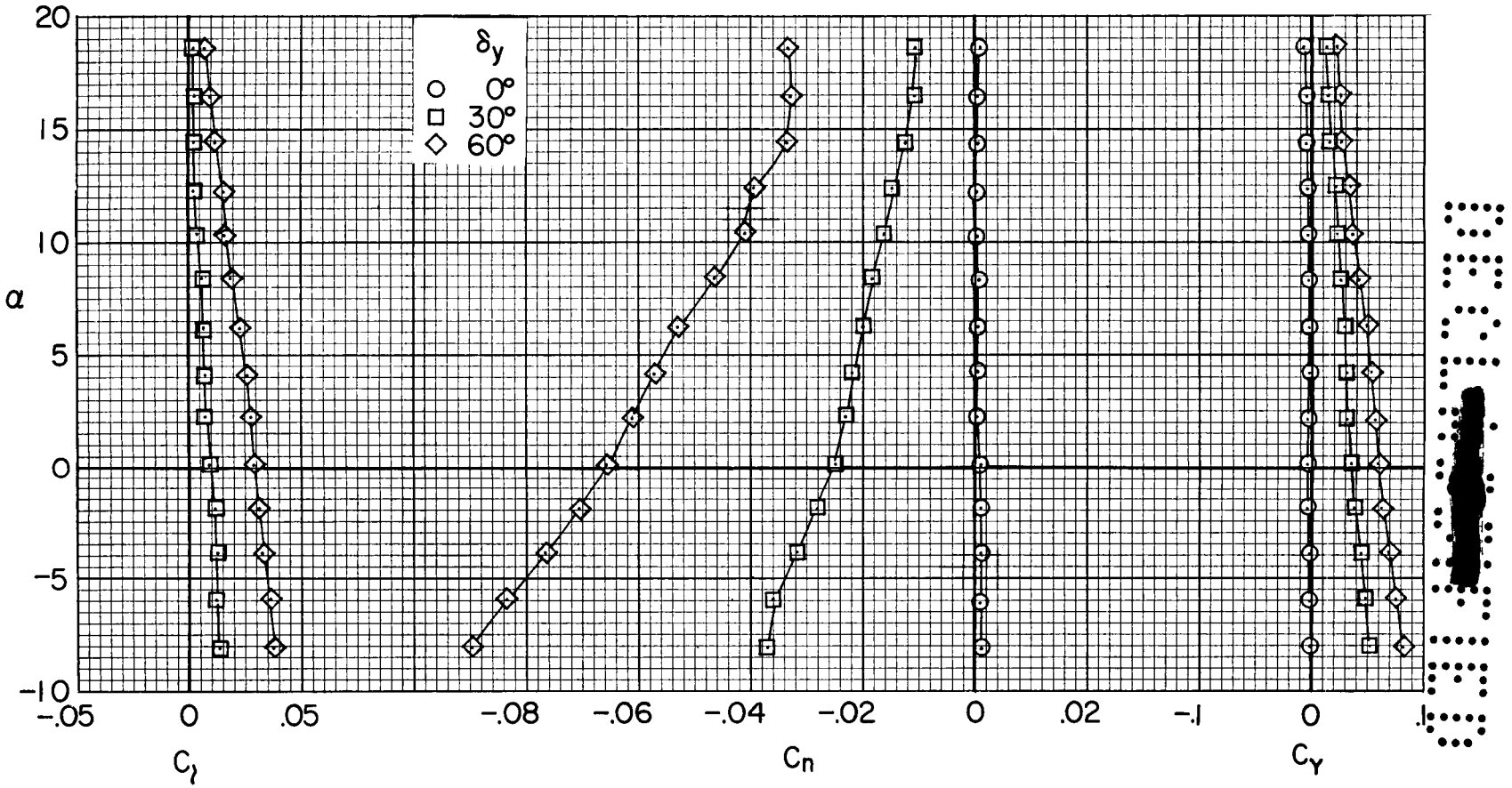

(a) Elevons on, $\delta_e = -10^\circ$.

Figure 9.- The effects of deflecting the left yaw flap on the lateral and directional characteristics of the basic model, for a range of angles of attack; $\beta = 0^\circ$, $R = 15 \times 10^6$, $M = 0.25$, $\delta_f = -10^\circ$, $\delta_p = 0^\circ$.

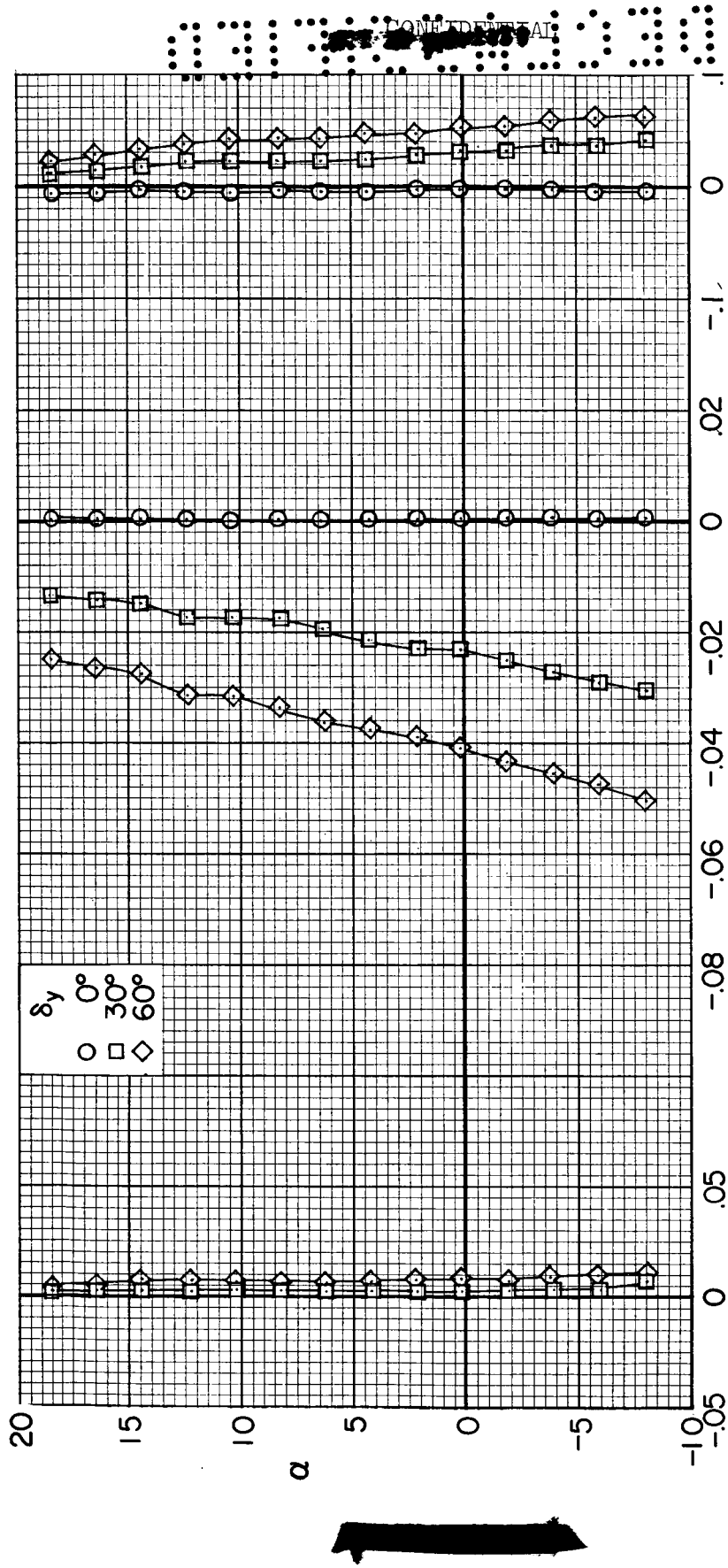

(b) Elevons off.

Figure 9.- Concluded.

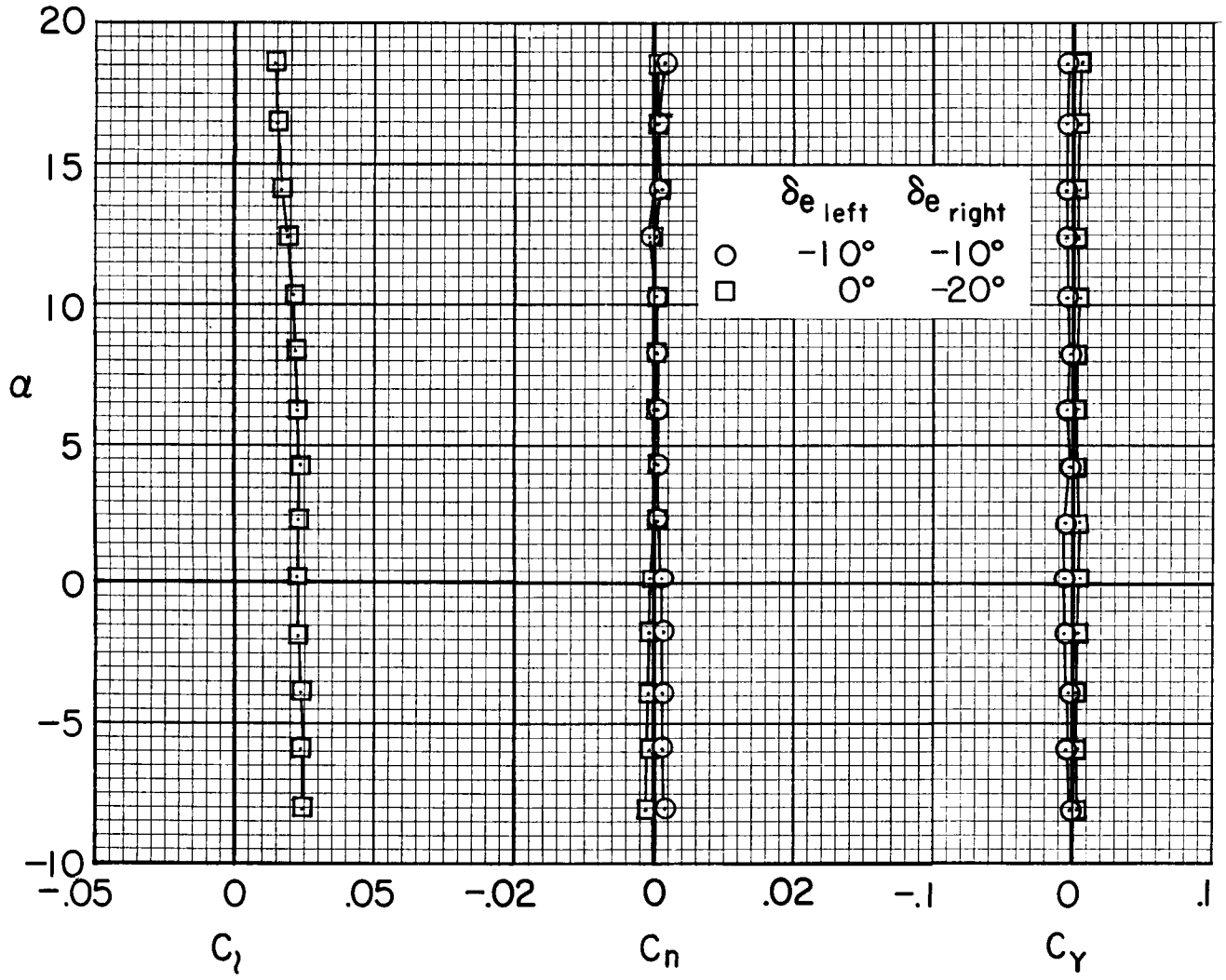

Figure 10.- The effects of deflecting the elevons asymmetrically on the lateral and directional characteristics of the basic model; $\beta = 0^\circ$, $R = 15 \times 10^6$, $M = 0.25$, $\delta_f = -10^\circ$, $\delta_p = 0^\circ$.

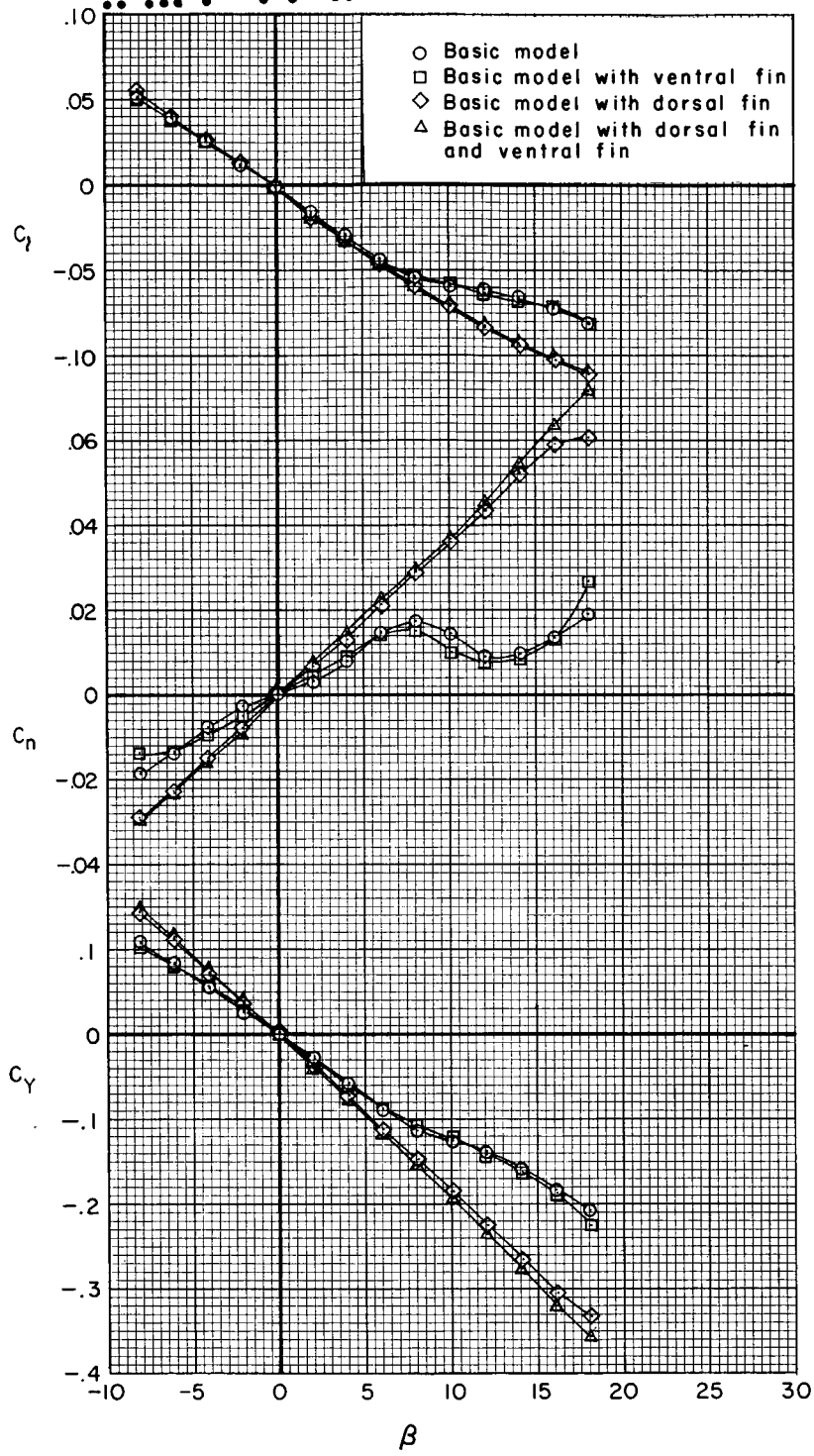

(a) M = 0.60

Figure 11.- The lateral and directional characteristics of the model at several Mach numbers, for a range of sideslip angles; $\alpha = 6^{\circ}$, $R = 5 \times 10^{6}$, $\delta_e = -10^{\circ}$, $\delta_p = 30^{\circ}$.

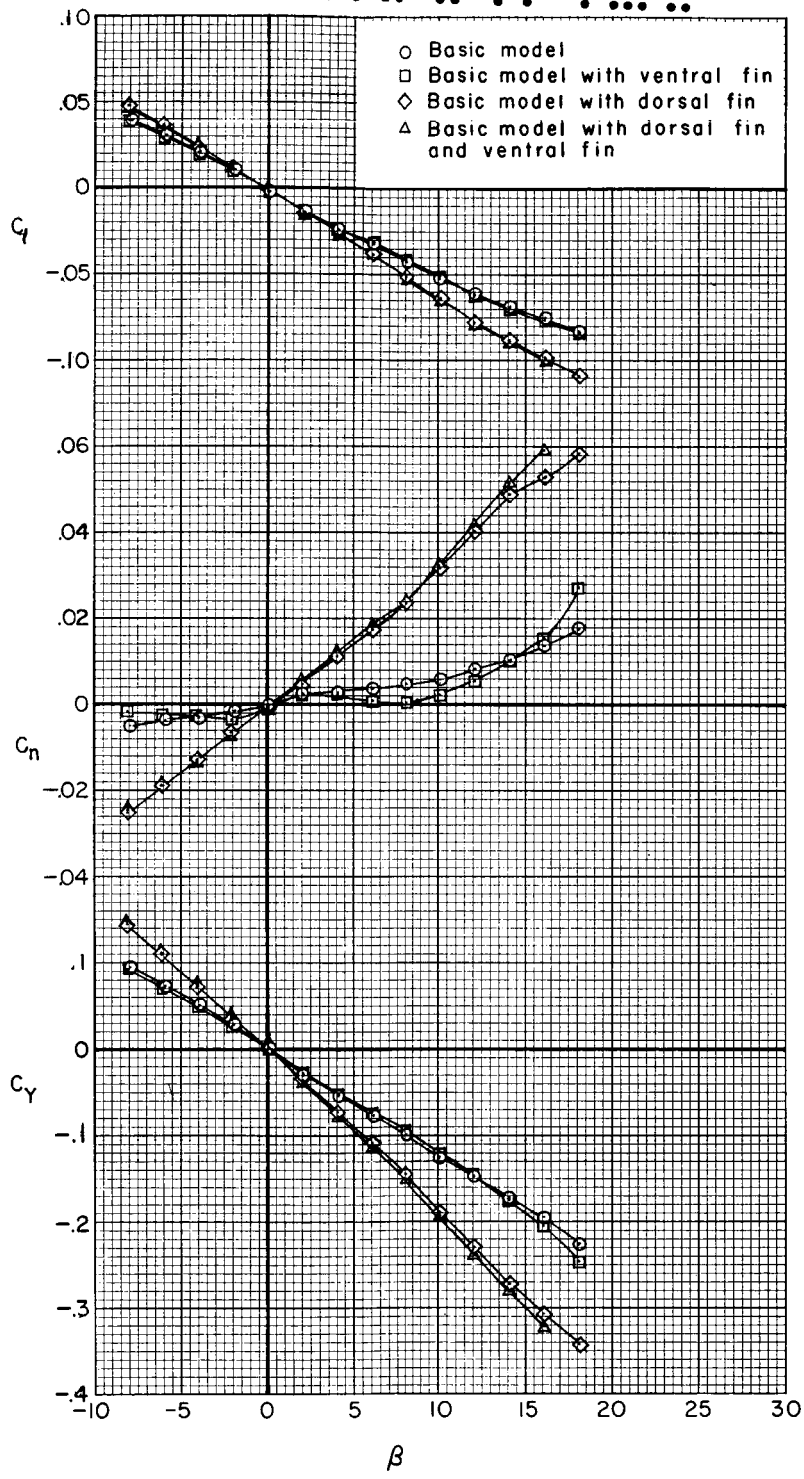

(b) M = 0.70

Figure 11.- Continued.

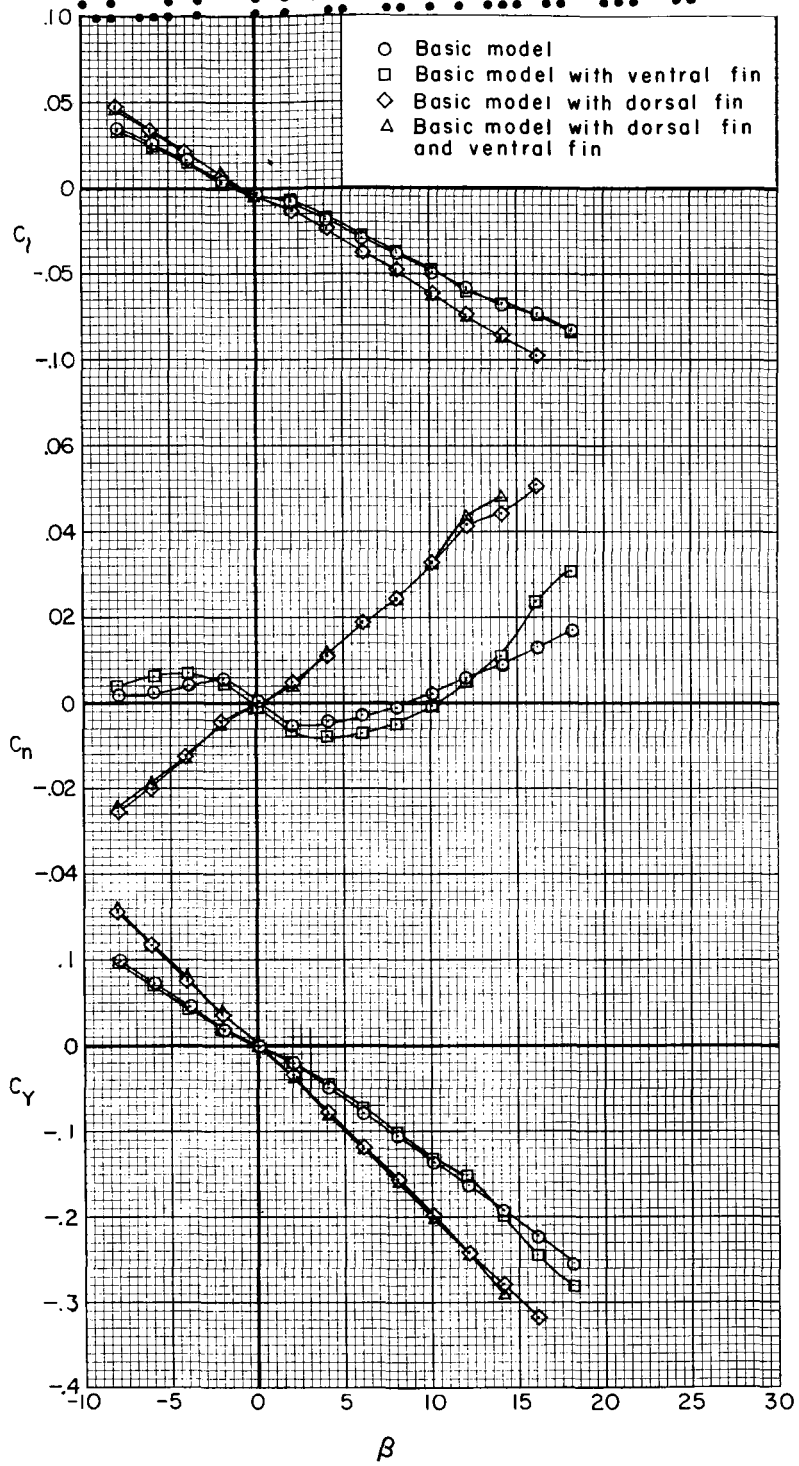

(c) M = 0.80

Figure 11.- Continued.

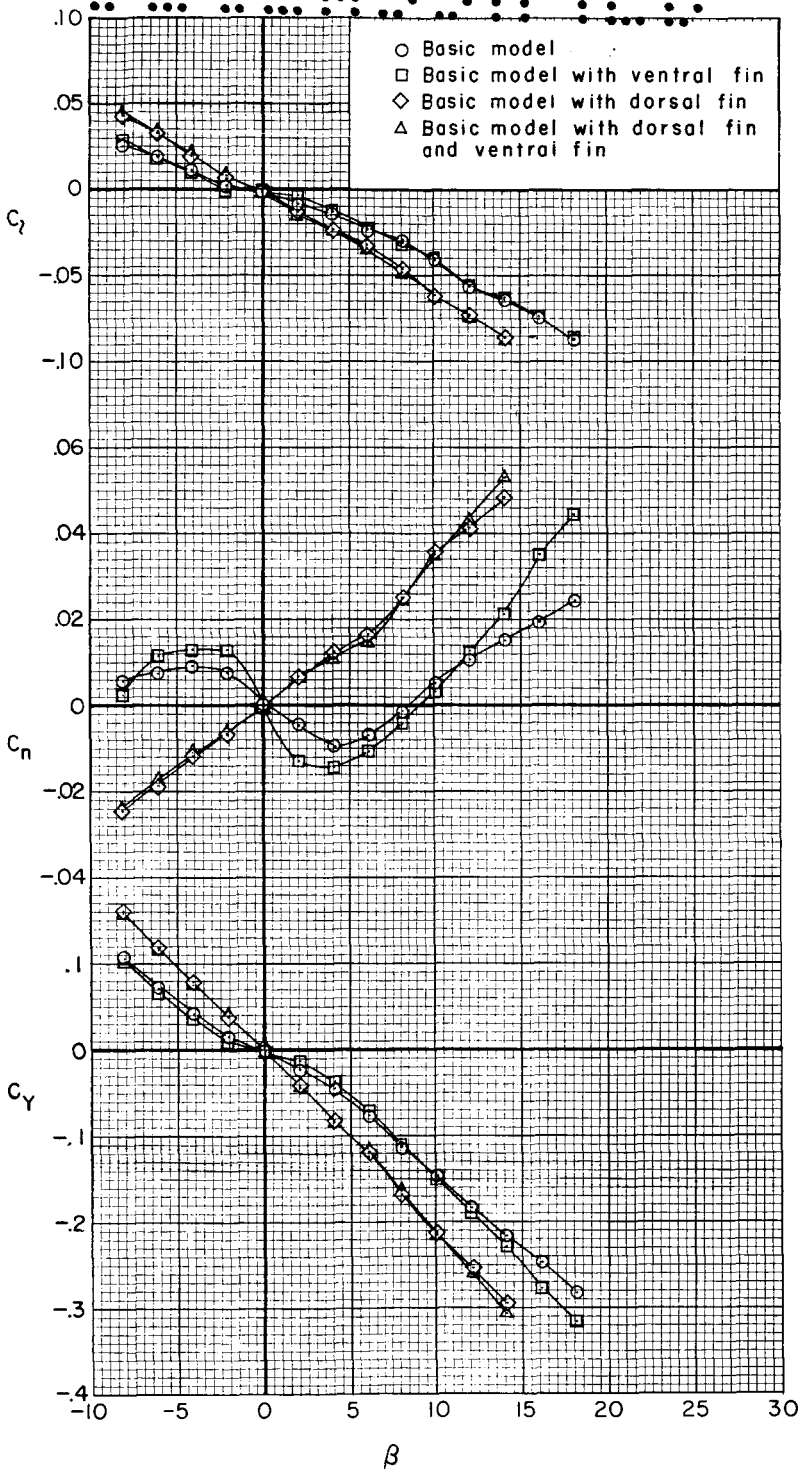

(d) M = 0.85

Figure 11.- Continued.

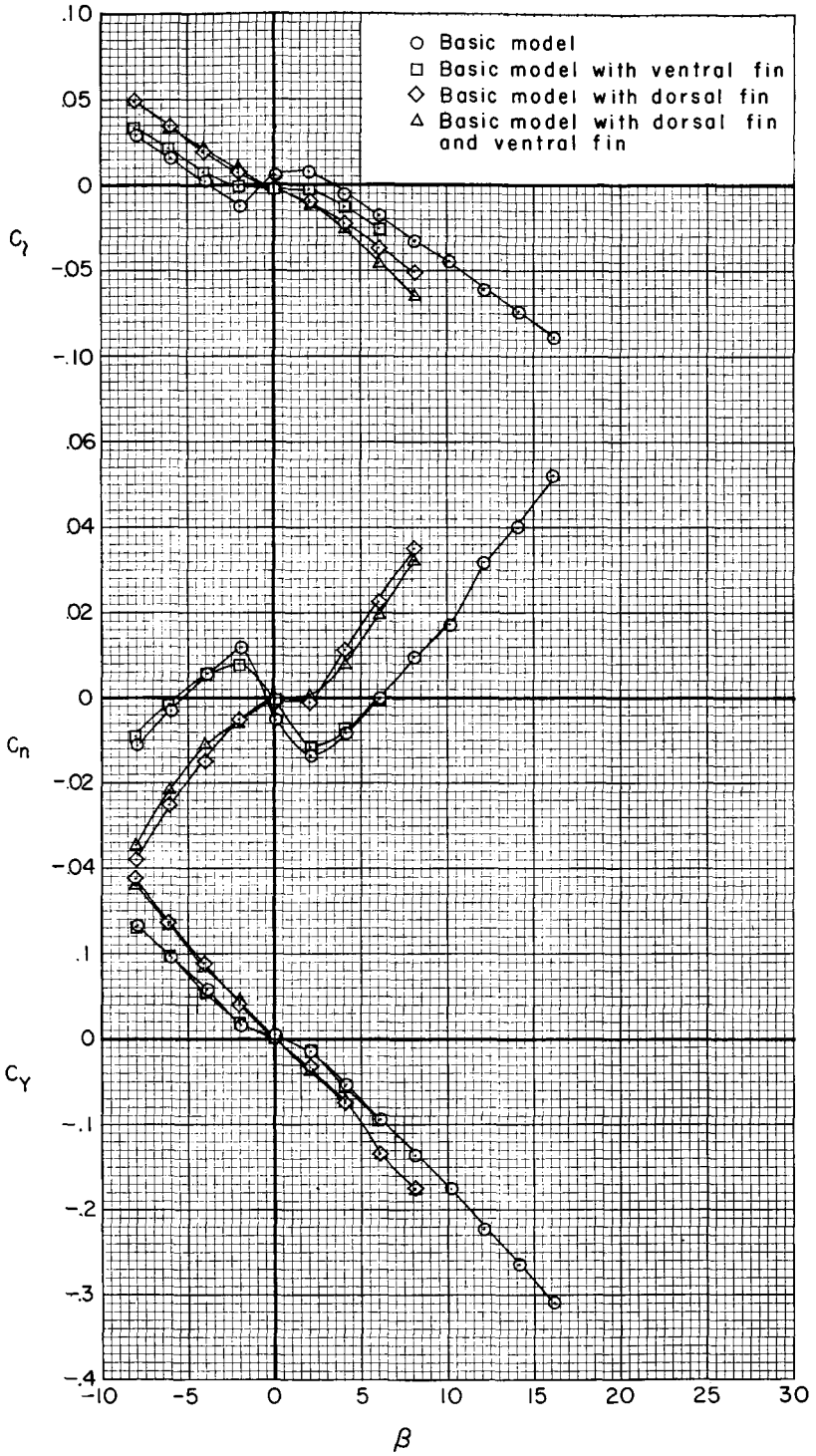

(e) M = 0.90

Figure 11.- Concluded.

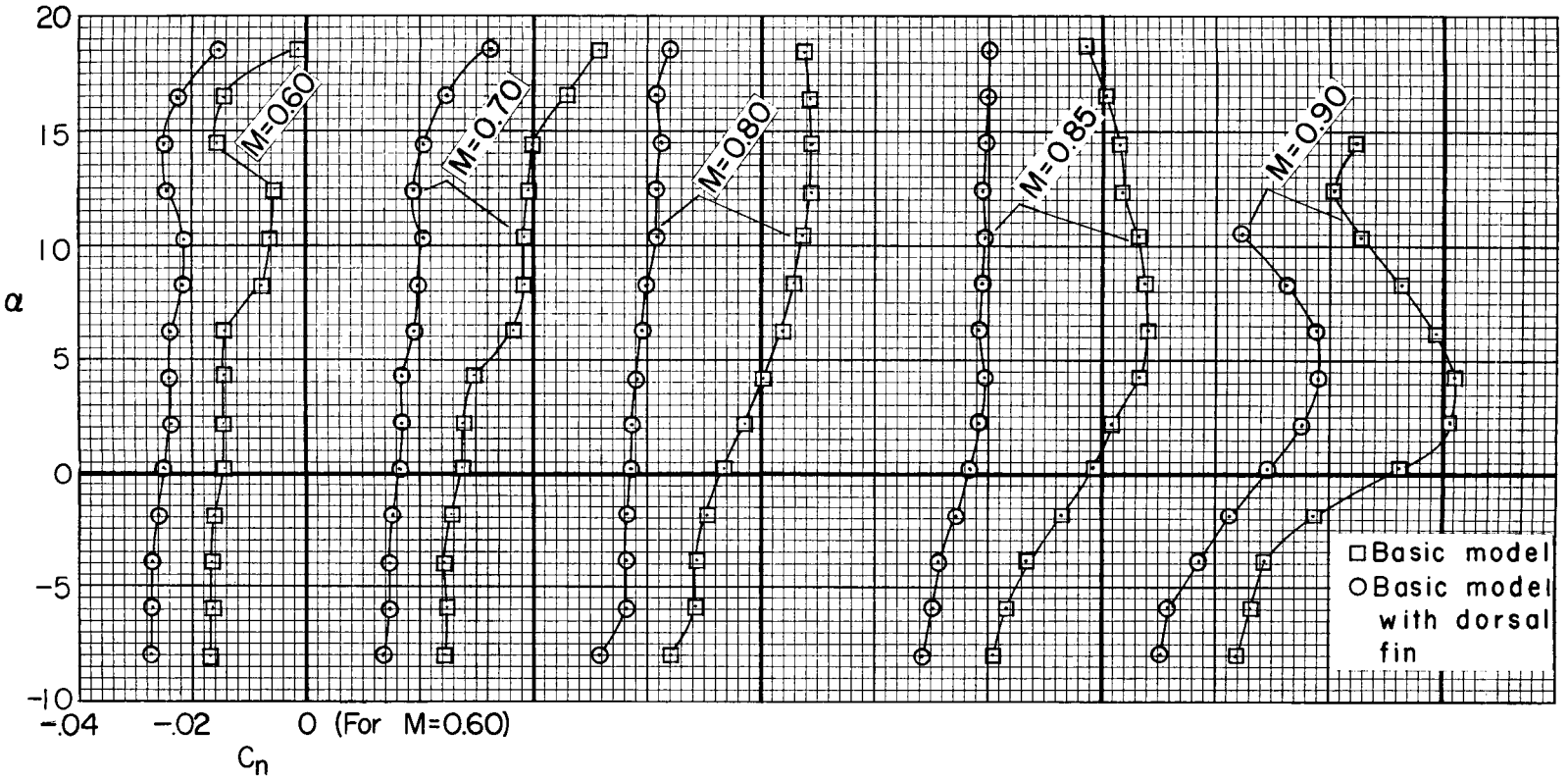

(a) Yawing moment.

Figure 12.- The lateral and directional characteristics of the model at several Mach numbers, for a range of angles of attack; $\beta = -6^{\circ}$, $R = 5 \times 10^{6}$, $\delta_e = -10^{\circ}$, $\delta_p = 30^{\circ}$.

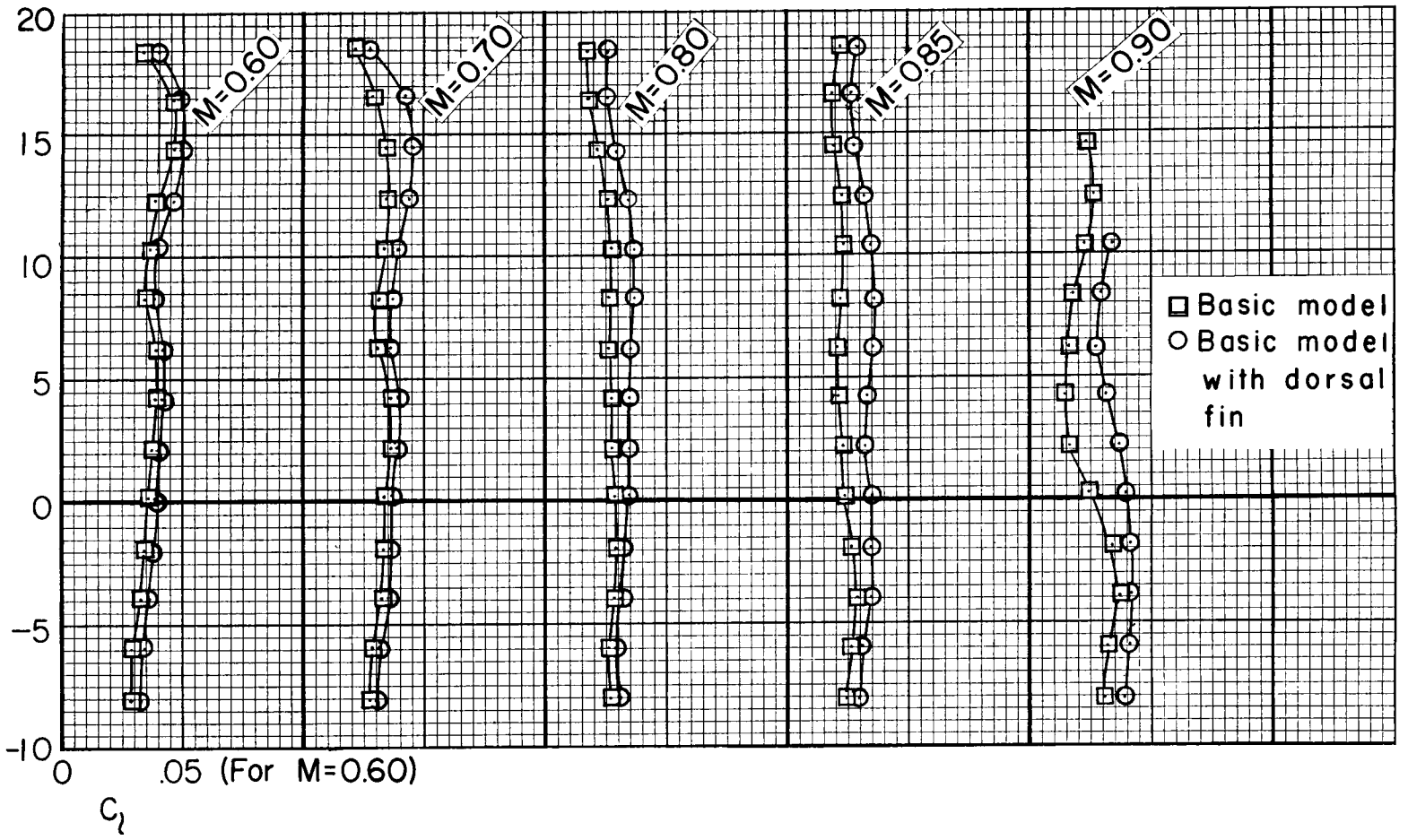

(b) Rolling moment.

Figure 12.- Continued.

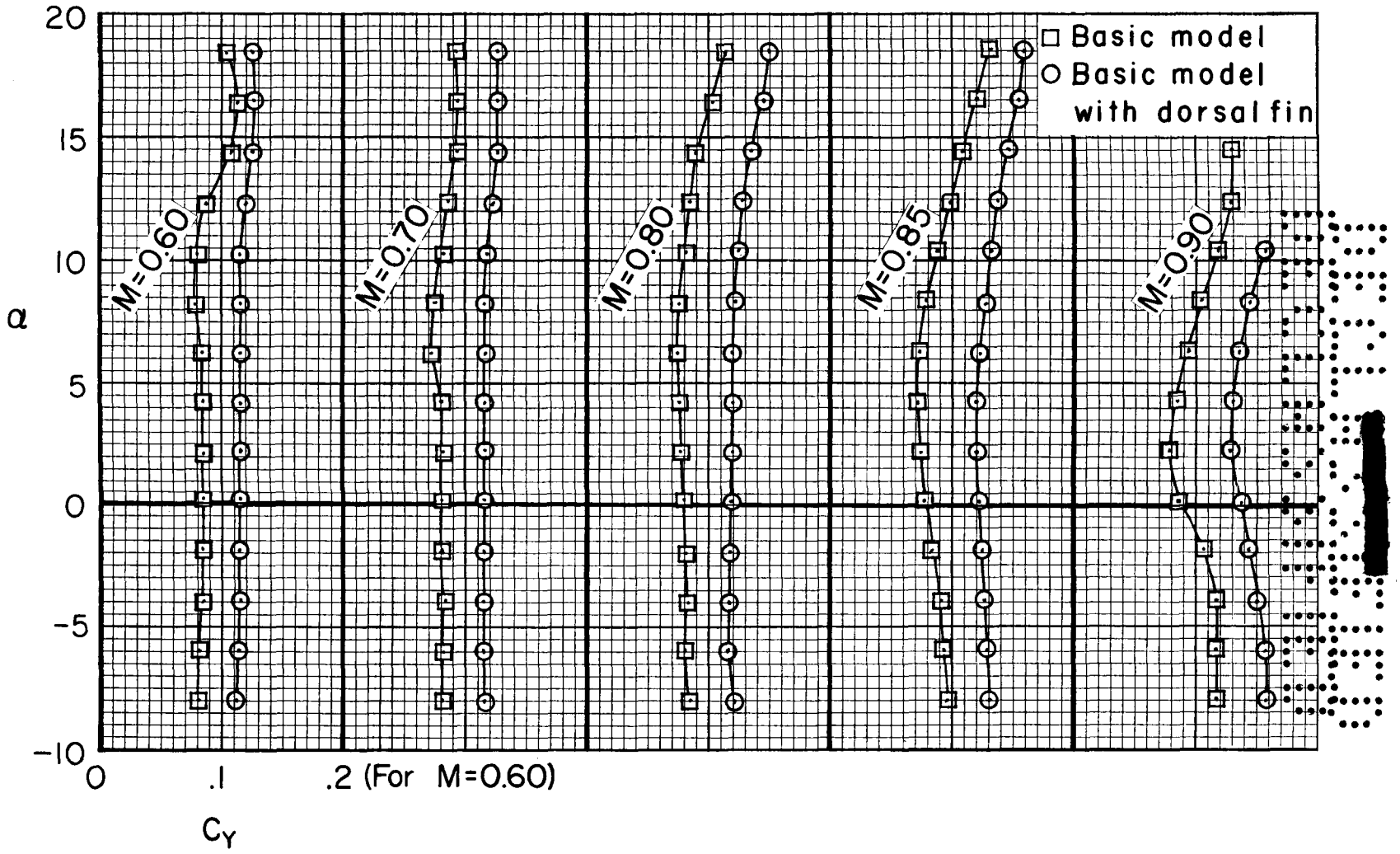

(c) Side force.

Figure 12.- Concluded.

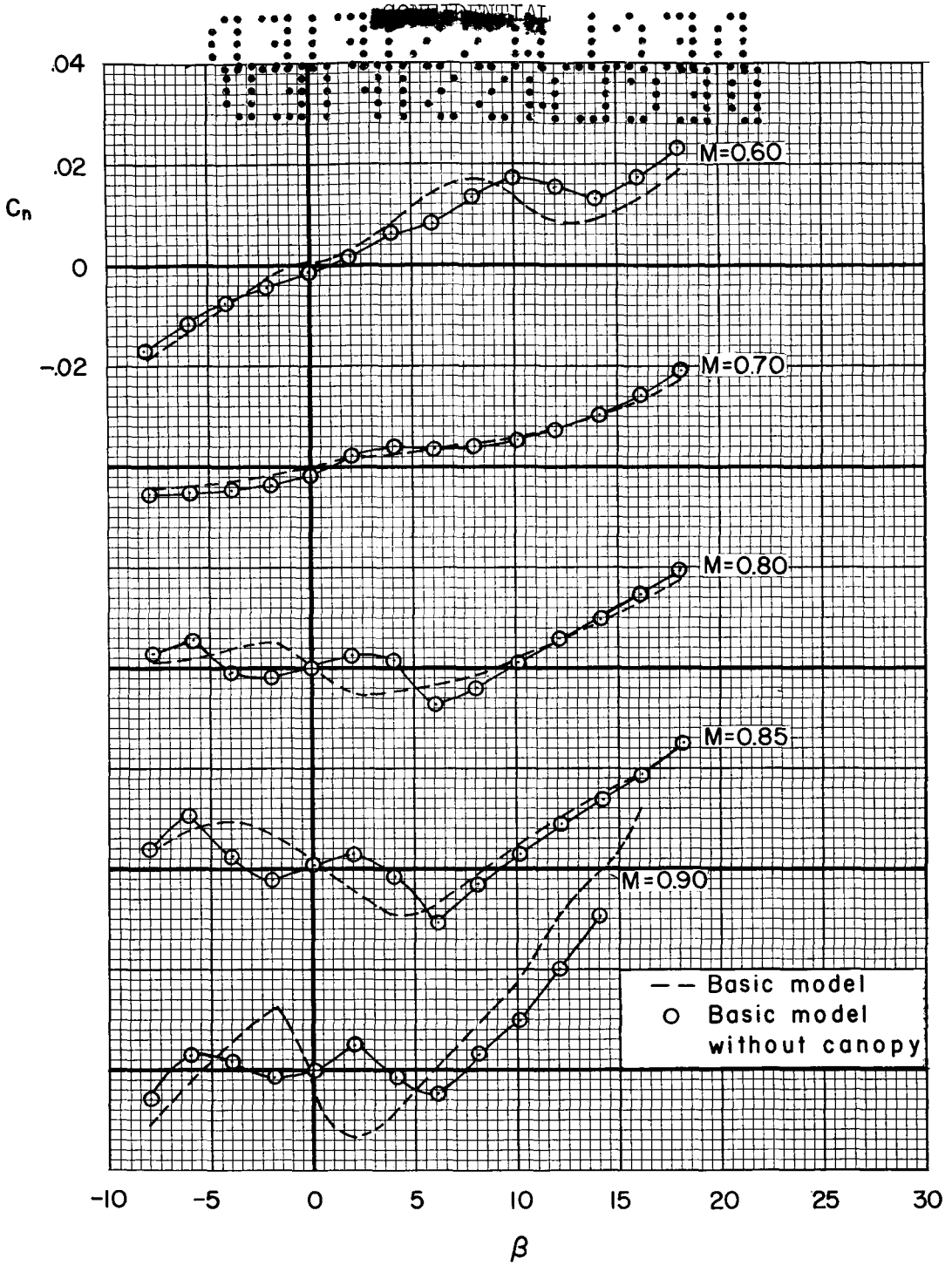

(a) Yawing moment.

Figure 13.- The effects of removing the canopy on the lateral and directional characteristics of the model at several Mach numbers; $\alpha = 6^{\circ}$, $R = 5 \times 10^{6}$, $\delta_e = -10^{\circ}$, $\delta_p = 30^{\circ}$.

[redacted]

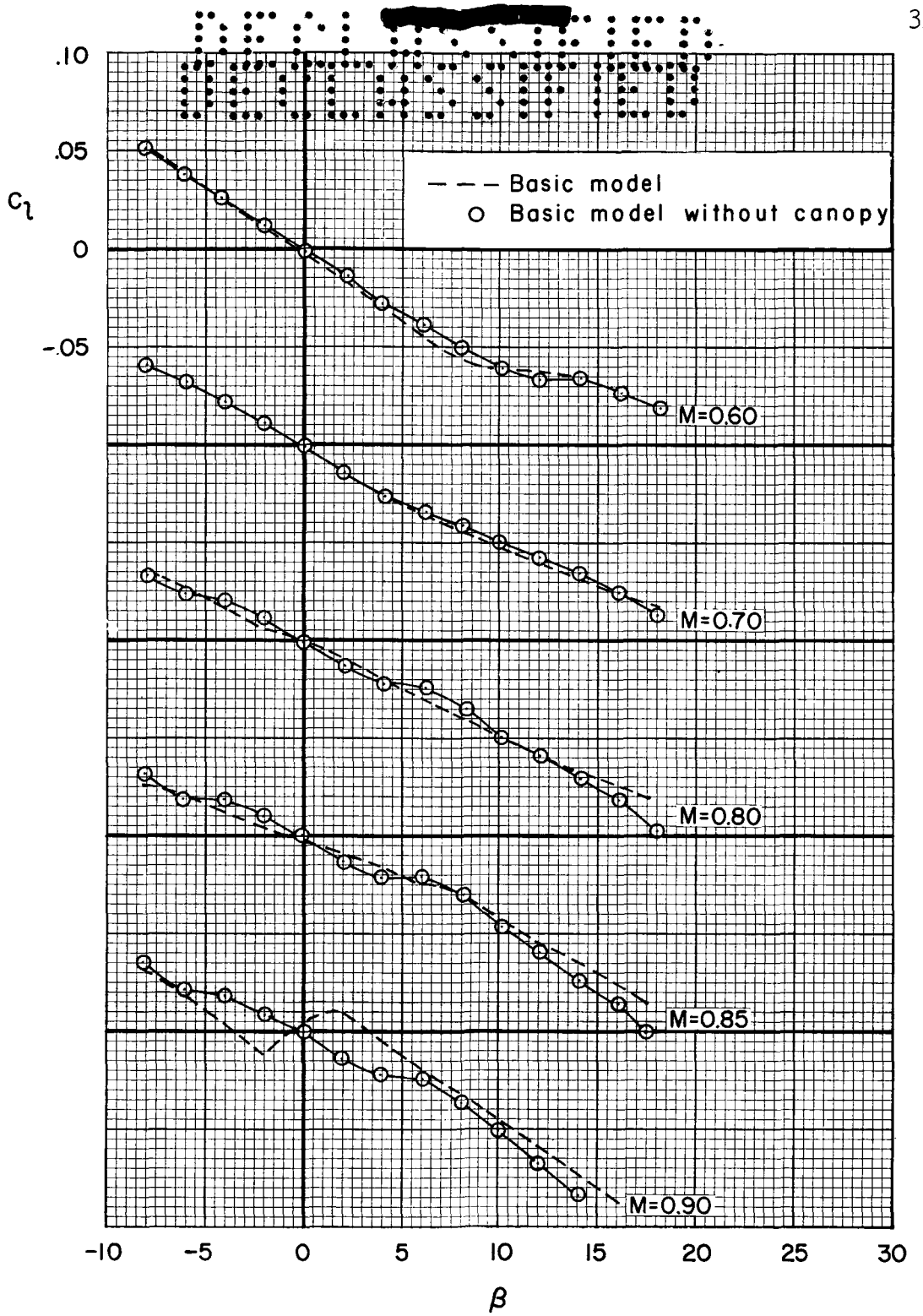

(b) Rolling moment.

Figure 13.- Continued.

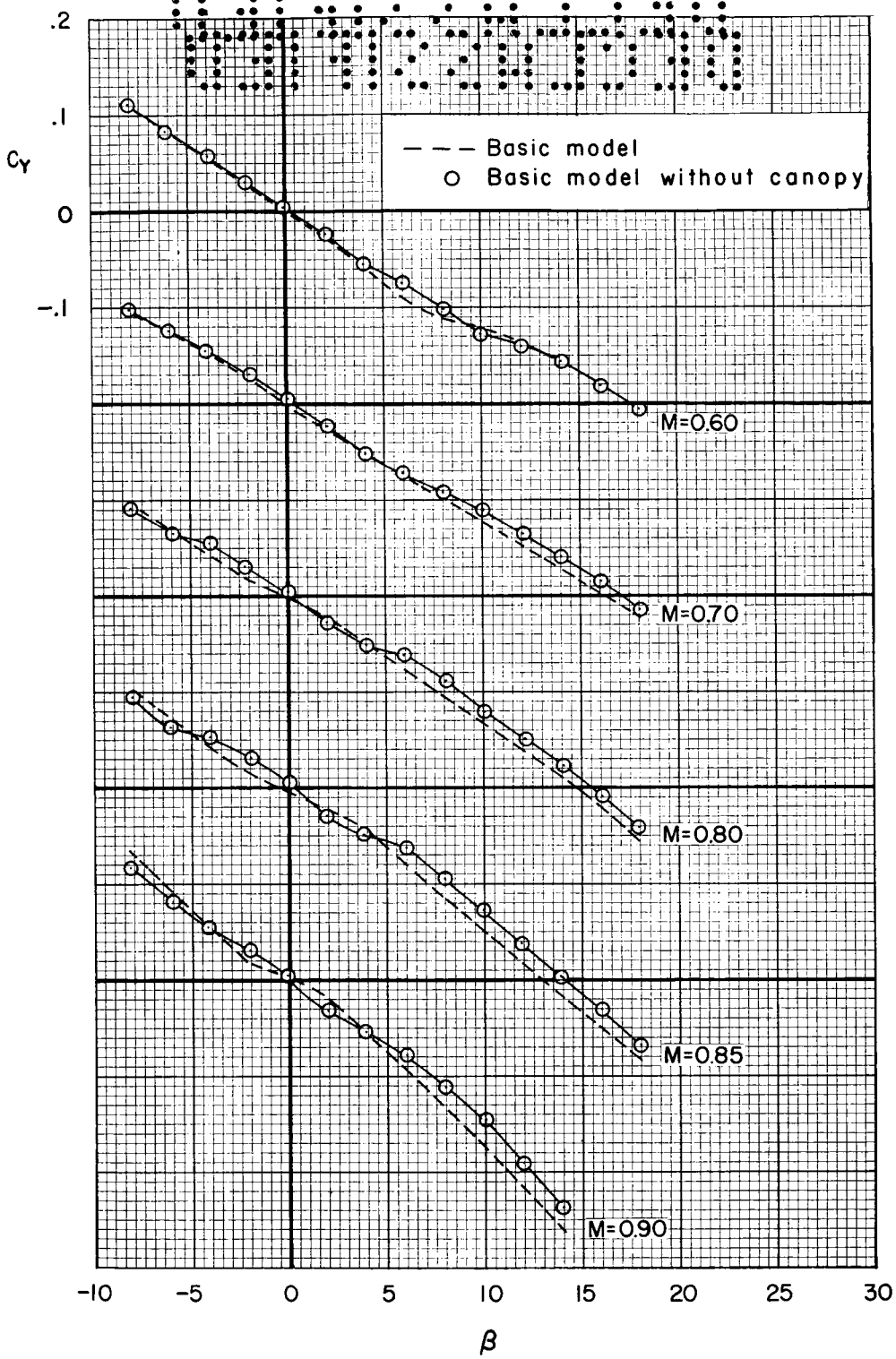

(c) Side force.

Figure 13.- Concluded.

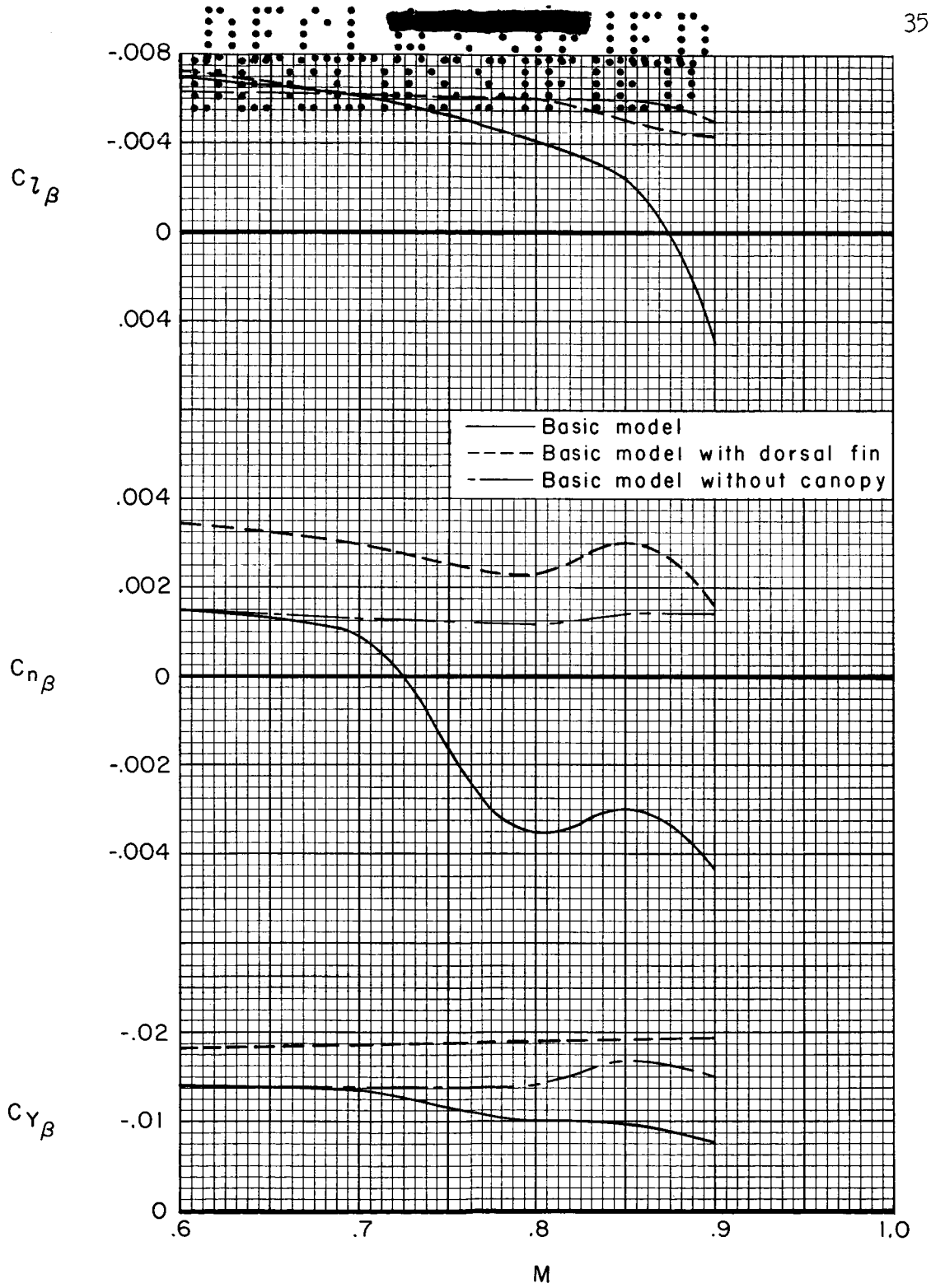

Figure 14.- The effects of Mach number on the lateral and directional stability derivatives of the model, evaluated at 0° sideslip angle; $\alpha = 6^\circ$, $R = 5\times10^6$, $\delta_e = -10^\circ$, $\delta_p = 30^\circ$.

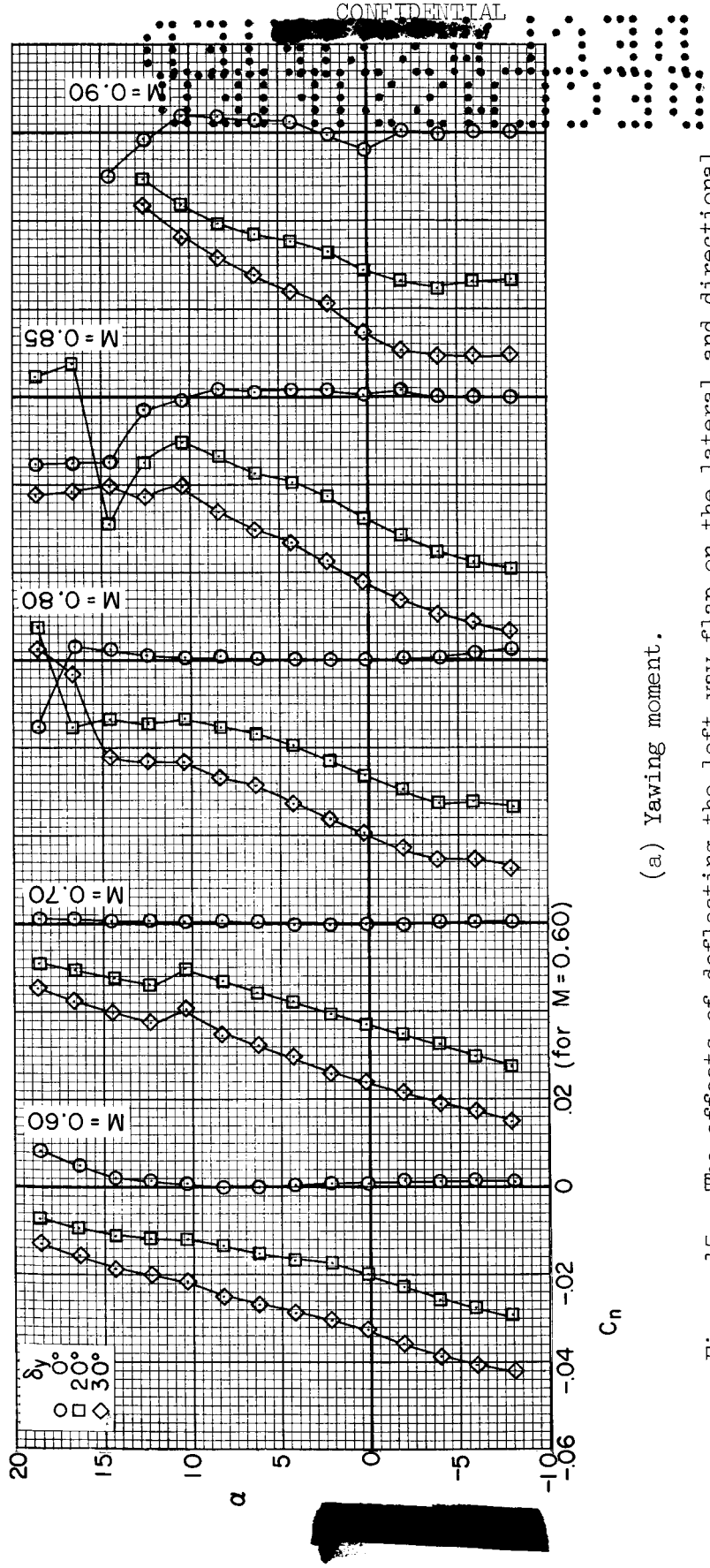

(a) Yawing moment.

Figure 15.- The effects of deflecting the left yaw flap on the lateral and directional characteristics of the basic model at several Mach numbers; $\beta = 0^{\circ}$, $R = 5 \times 10^{6}$, $\delta_e = -10^{\circ}$, $\delta_p = 30^{\circ}$.

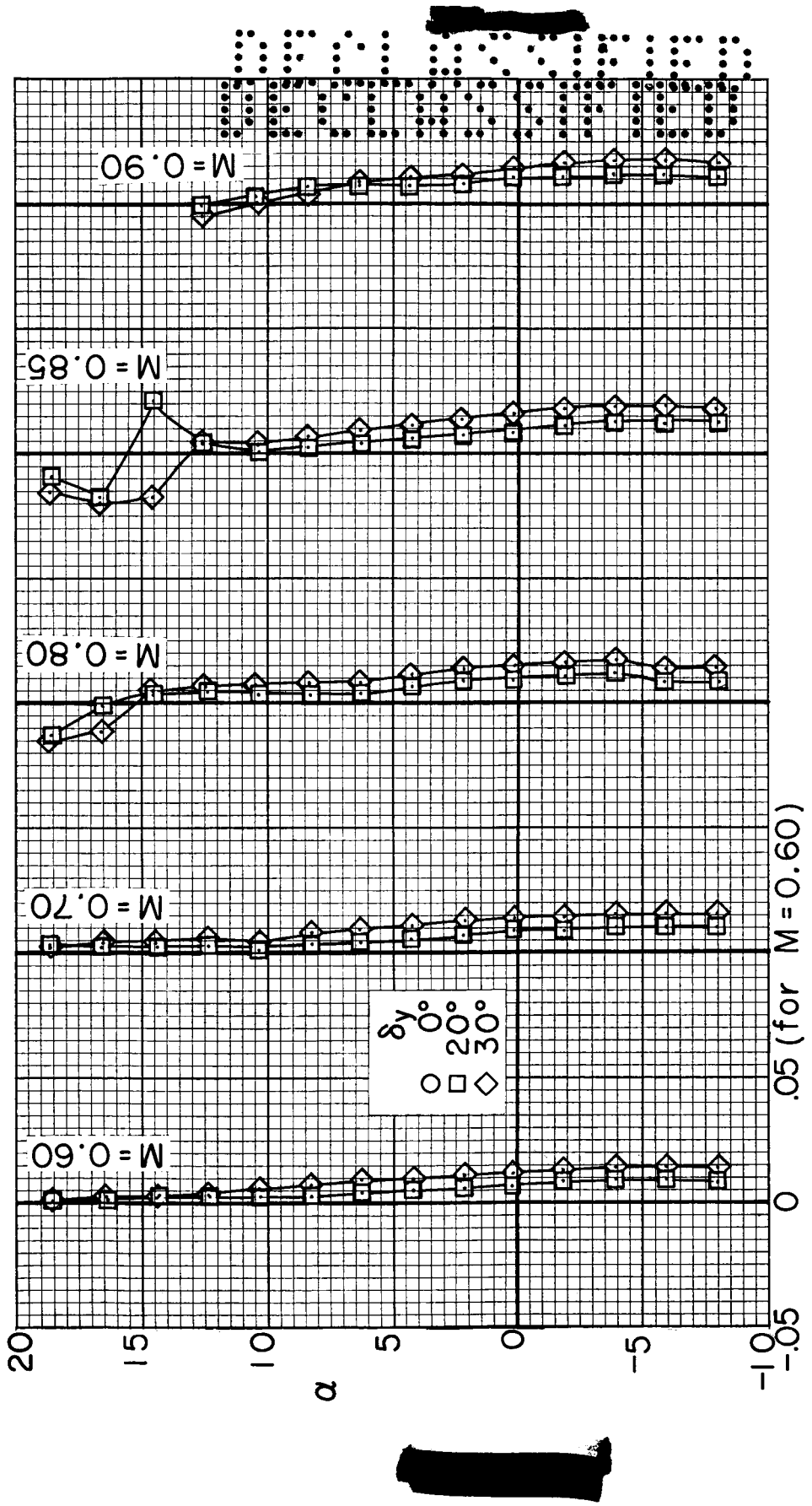

(b) Rolling moment.

Figure 15.- Continued.

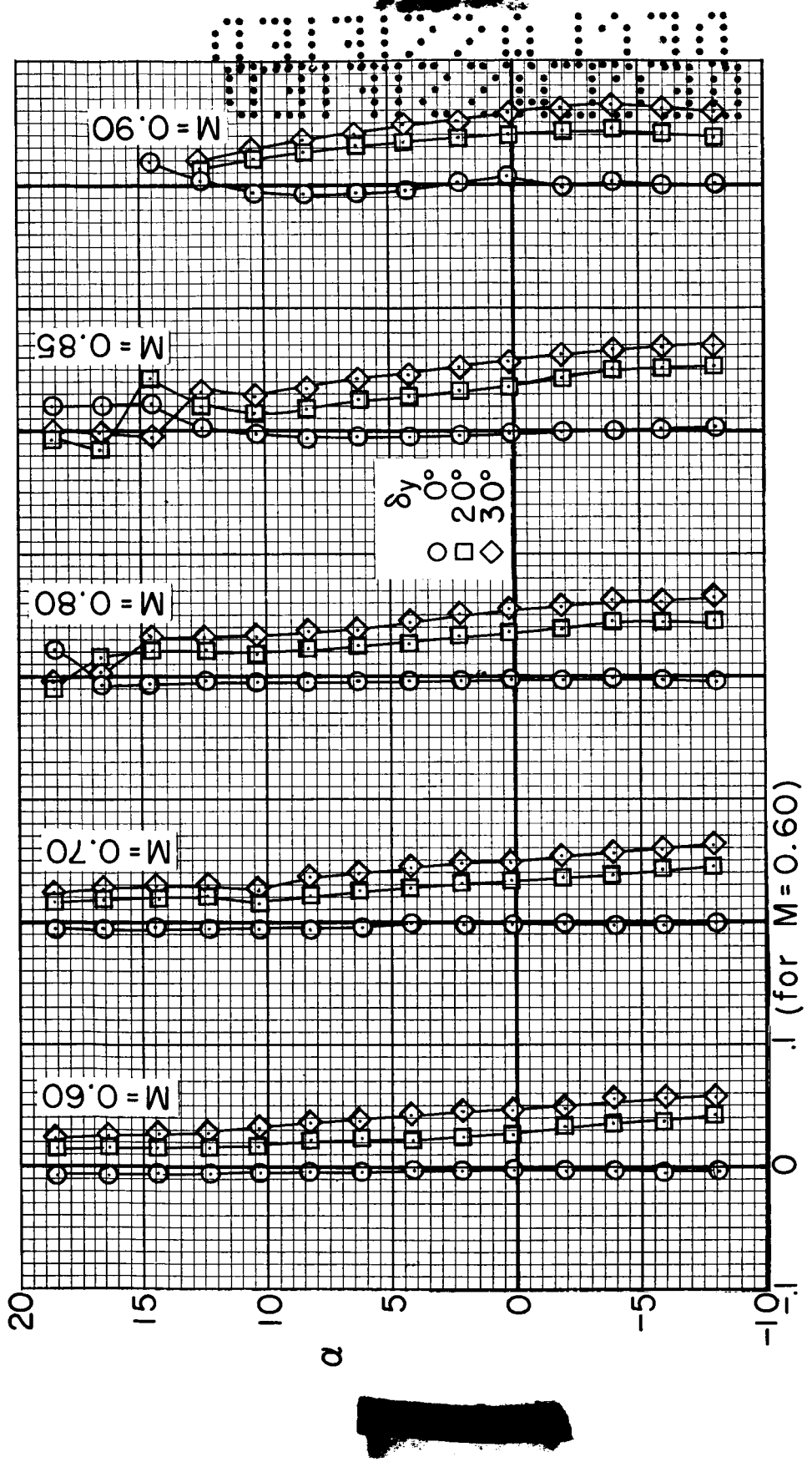

(c) Side force.

Figure 15.- Concluded.

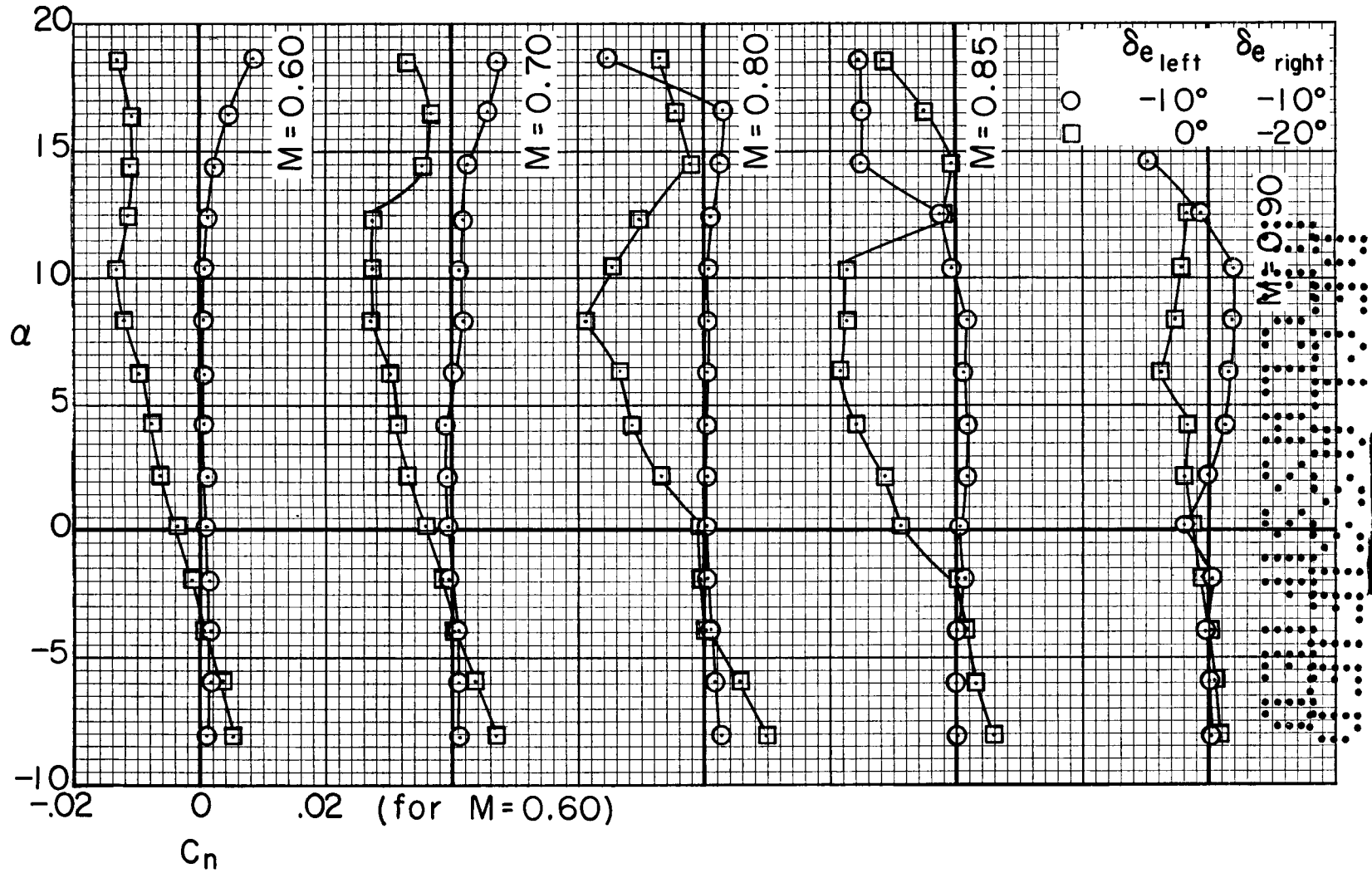

(a) Yawing moment.

Figure 16.- The effects of deflecting the elevons asymmetrically on the lateral and directional characteristics of the basic model at several Mach numbers; $\beta = 0^{\circ}$, $R = 5 \times 10^{6}$, $\delta_p = 30^{\circ}$.

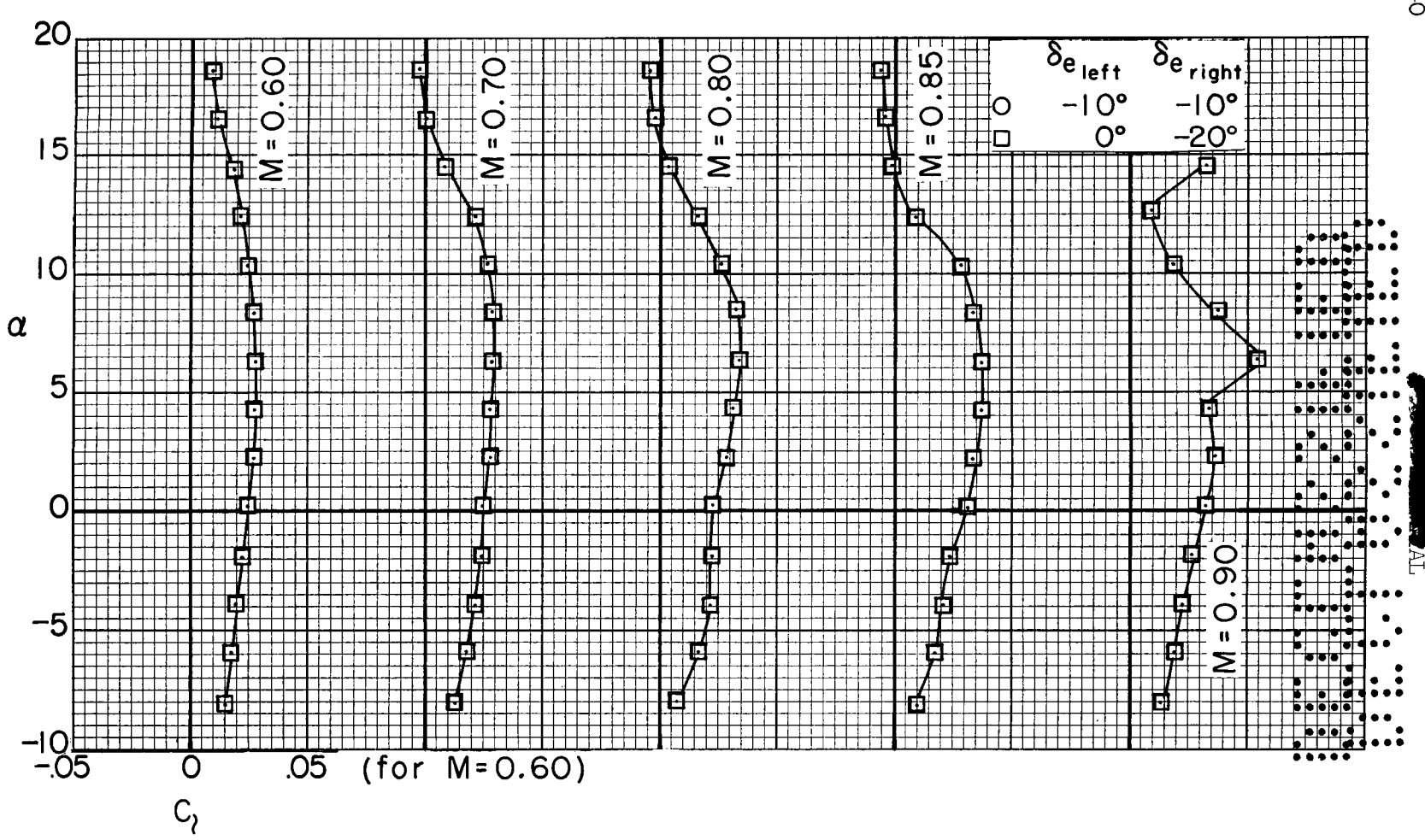

(b) Rolling moment.

Figure 16.- Continued.

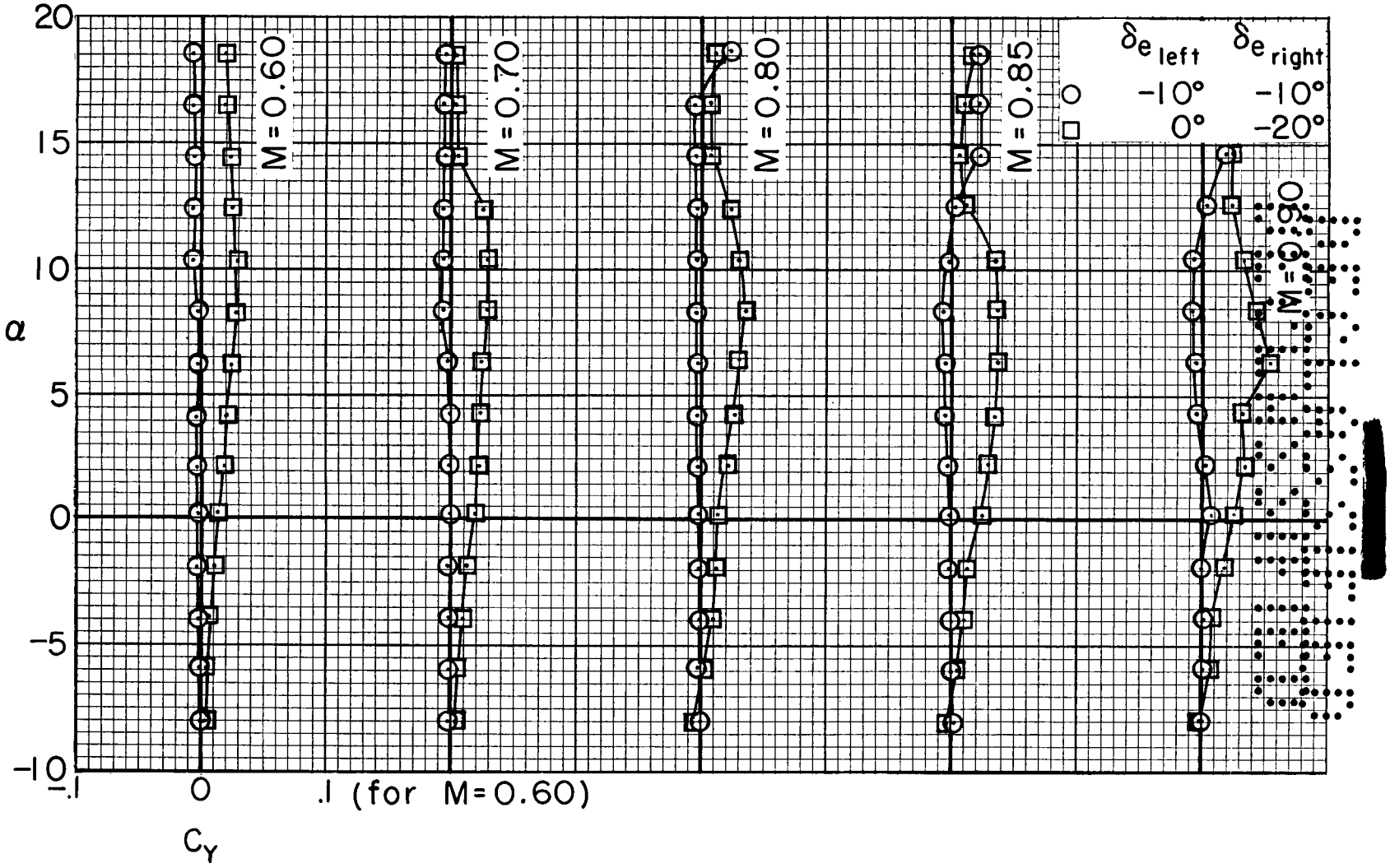

(c) Side force.

Figure 16.- Concluded.

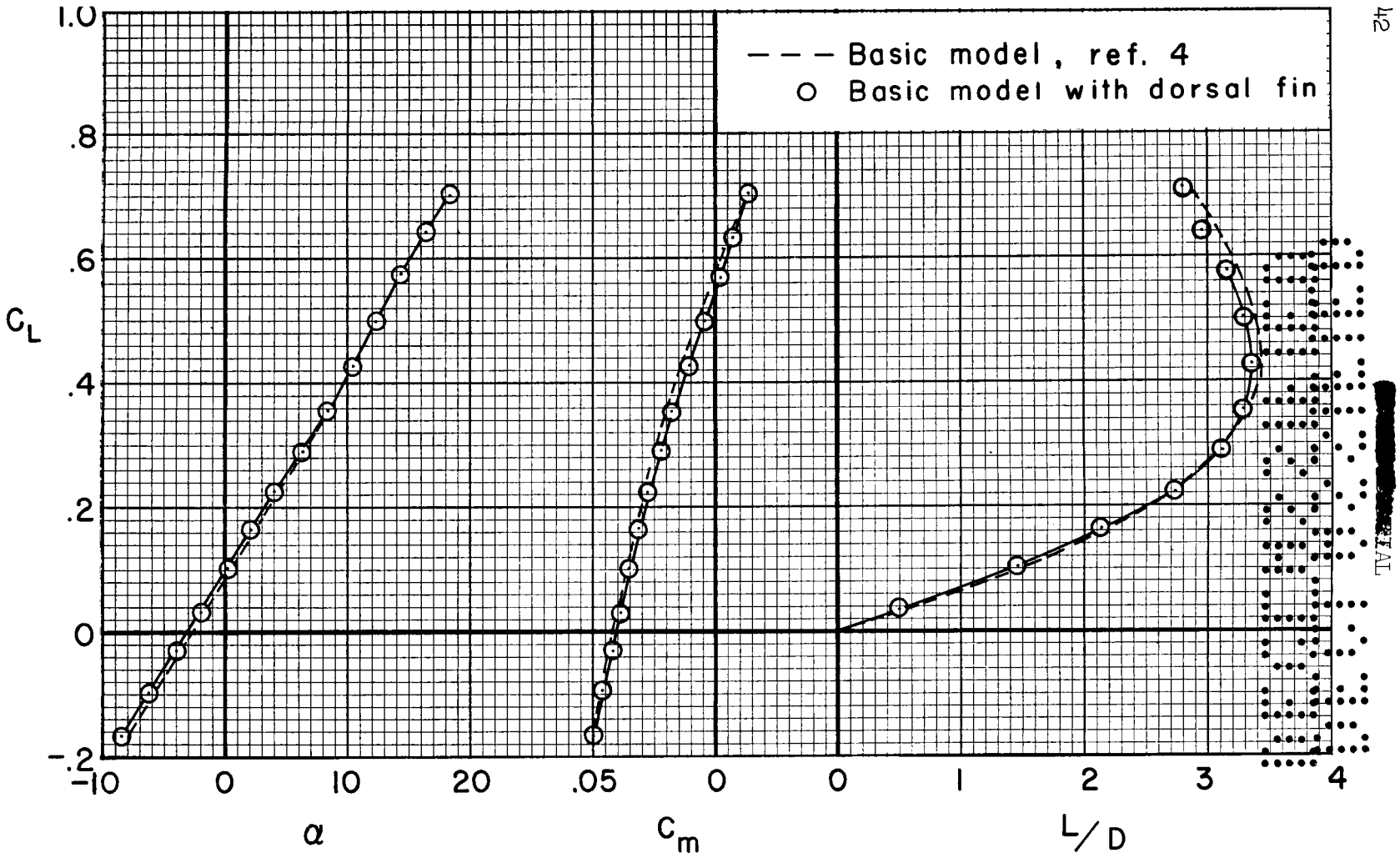

Figure 17.- The effects of the dorsal fin on the longitudinal characteristics of the model at a Mach number of 0.25; $R = 15 \times 10^6$, $\delta_e = -10^\circ$, $\delta_f = -10^\circ$, $\delta_p = 0^\circ$.

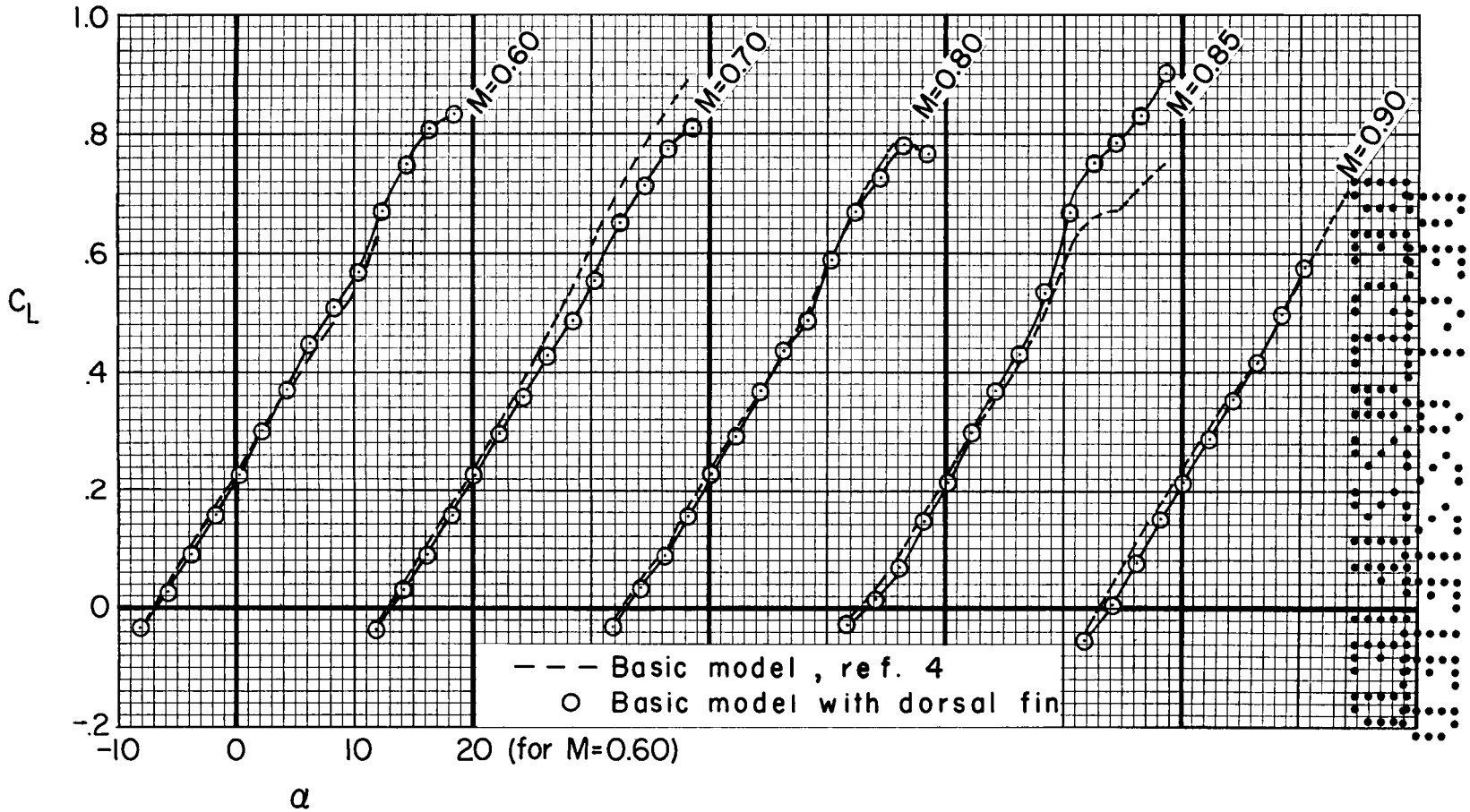

(a) Lift.

Figure 18.- The effects of the dorsal fin on the longitudinal characteristics of the model at several Mach numbers; $R = 5 \times 10^6$, $\delta_e = -10^\circ$, $\delta_p = 30^\circ$.

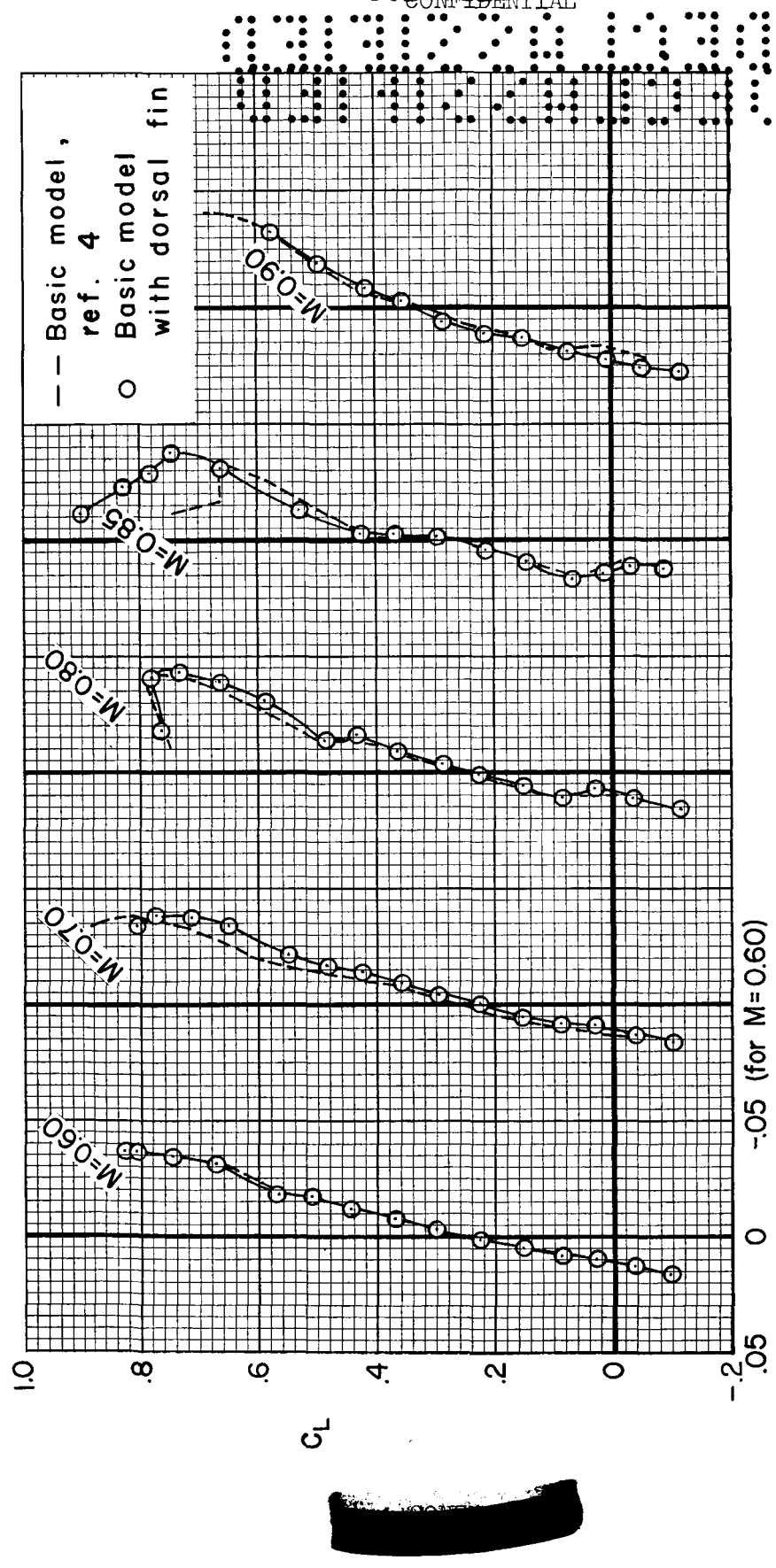

(b) Pitching moment.

Figure 18.- Continued.

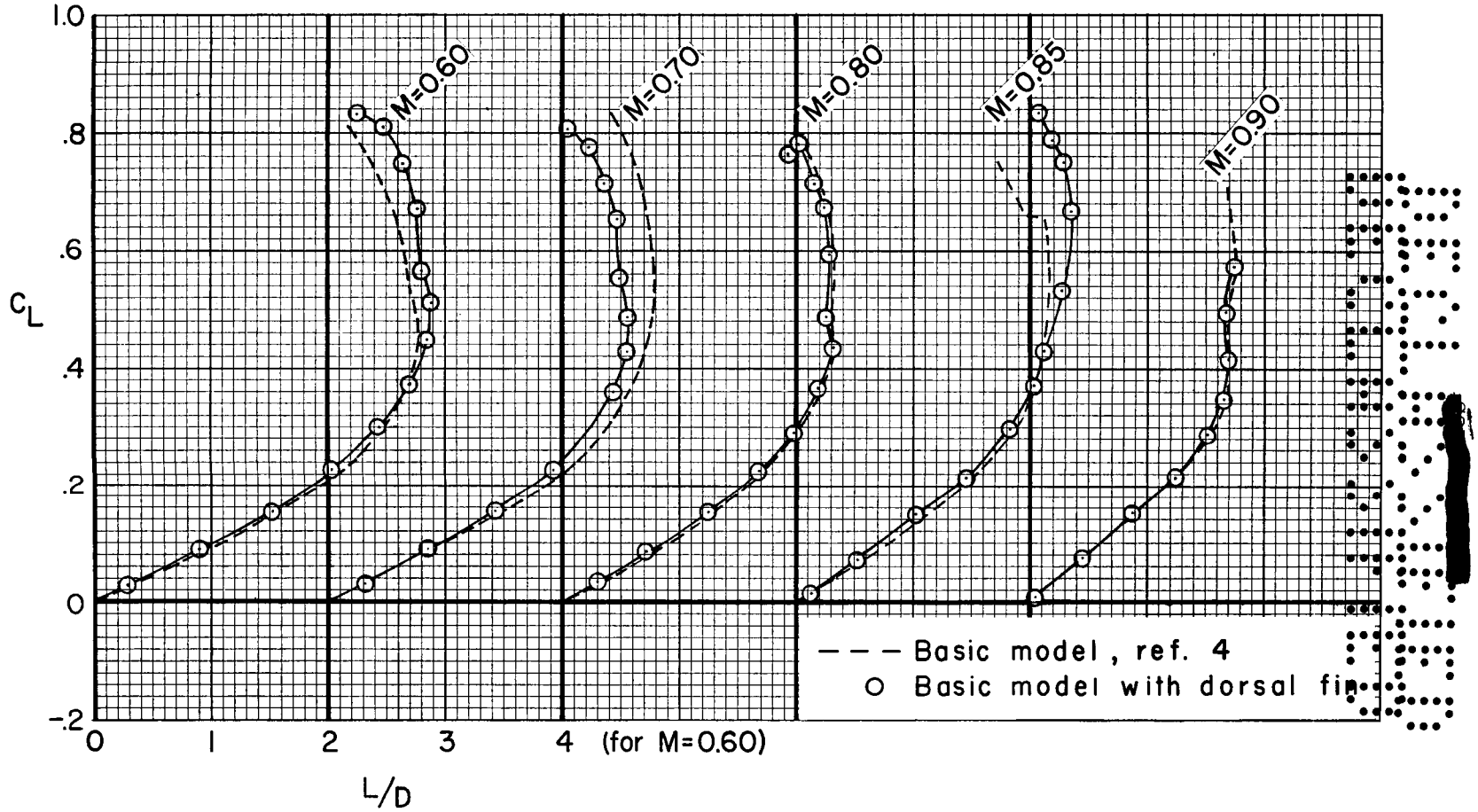

(c) Lift-drag ratio.

Figure 18.- Concluded.

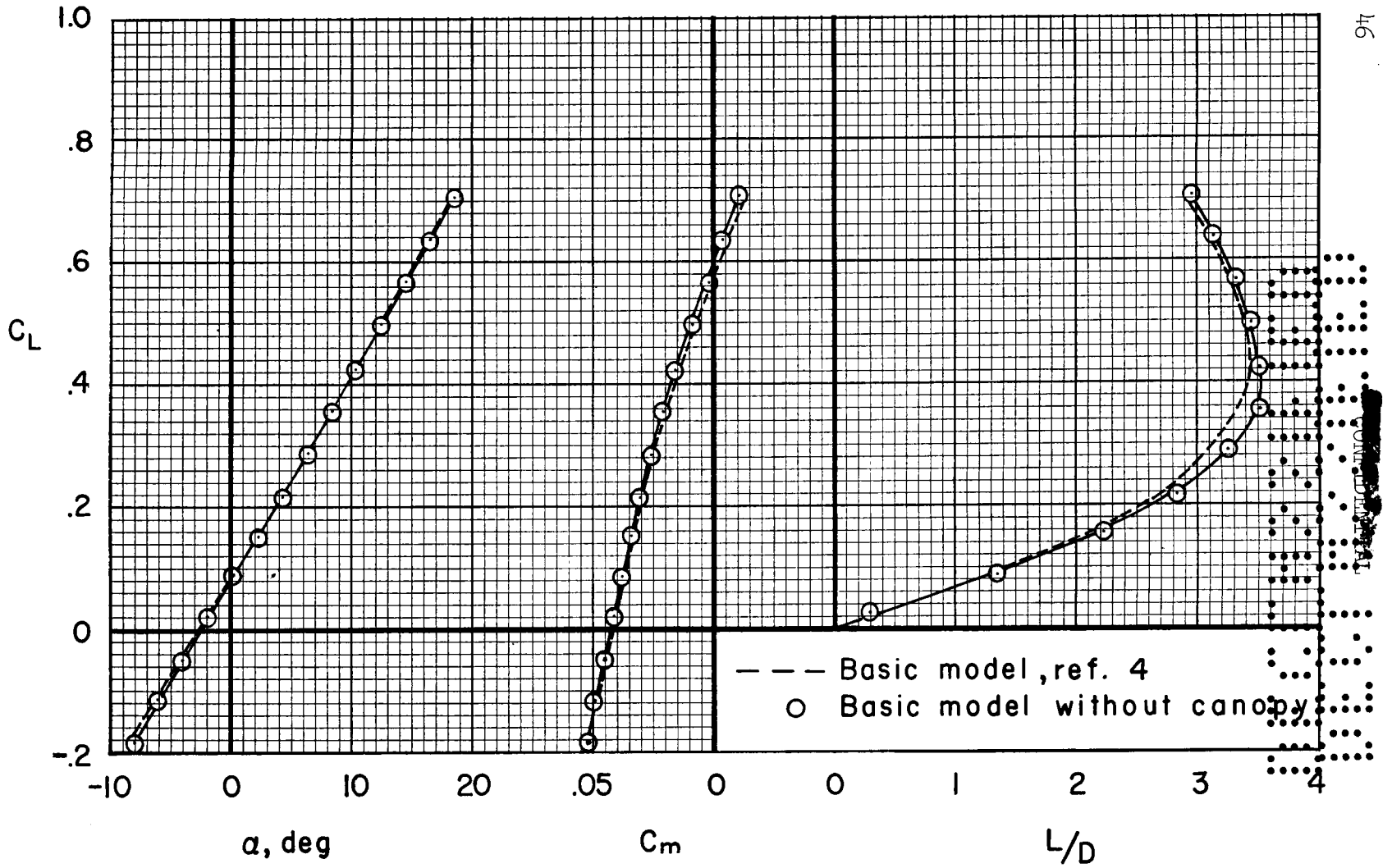

Figure 19.- The effects of removing the canopy on the longitudinal characteristics of the model at a Mach number of 0.25; $R = 15 \times 10^6$, $\delta_e = -10^\circ$, $\delta_f = -10^\circ$, $\delta_p = 0^\circ$.

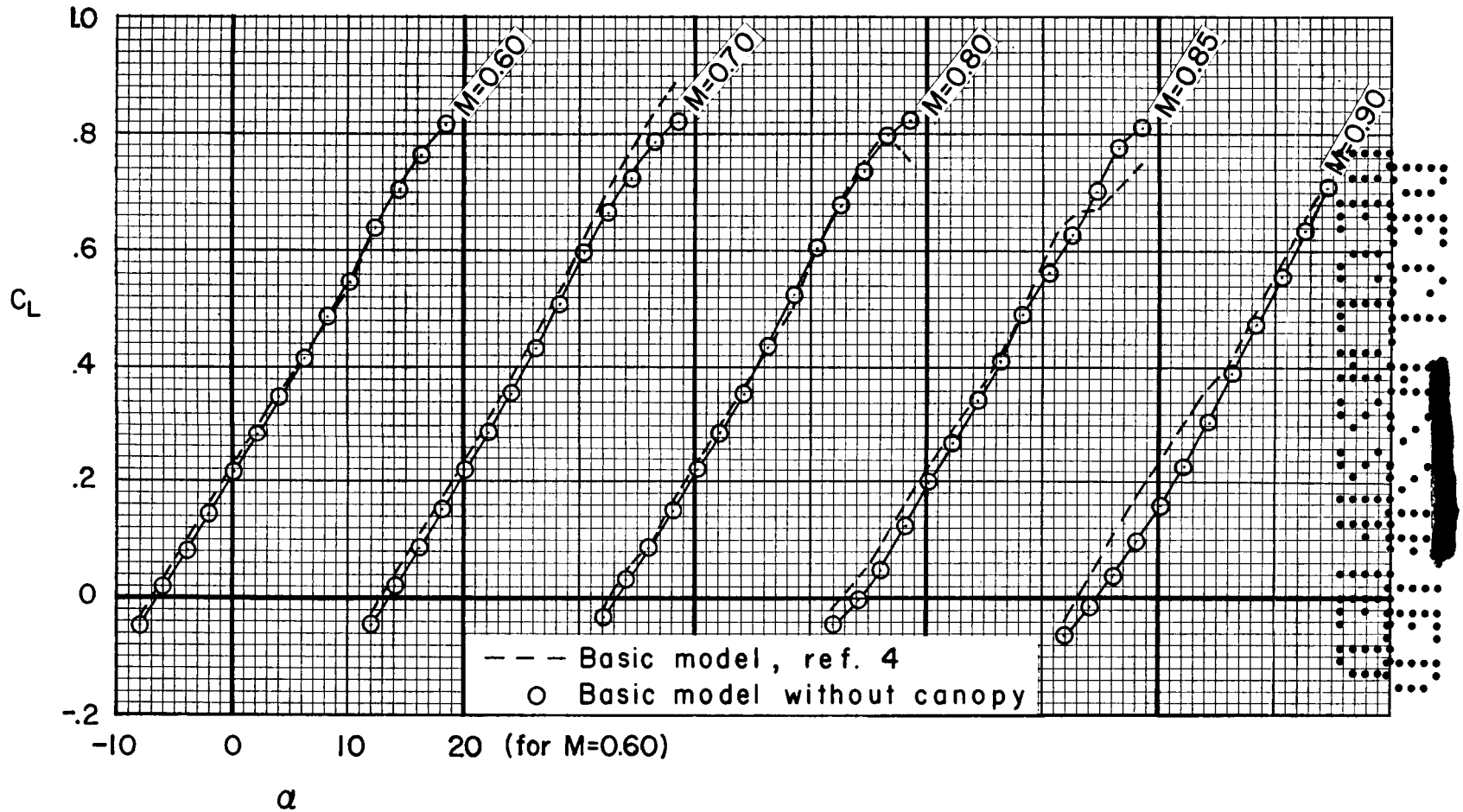

Figure 20.- The effects of removing the canopy on the longitudinal characteristics of the model at several Mach numbers; R = 5×10^6, $\delta_e = -10^\circ$, $\delta_p = 30^\circ$.

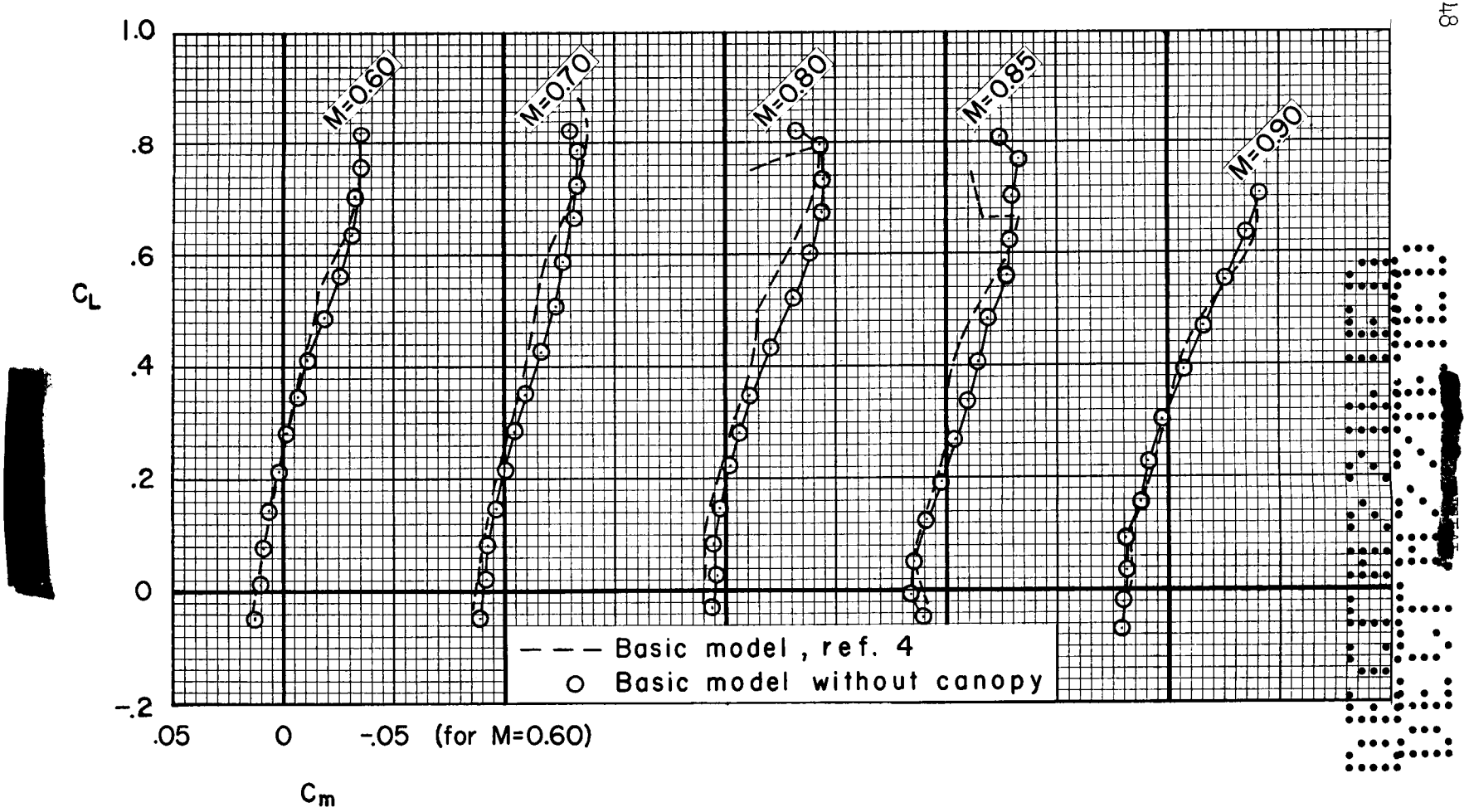

(b) Pitching moment.

Figure 20.- Continued.

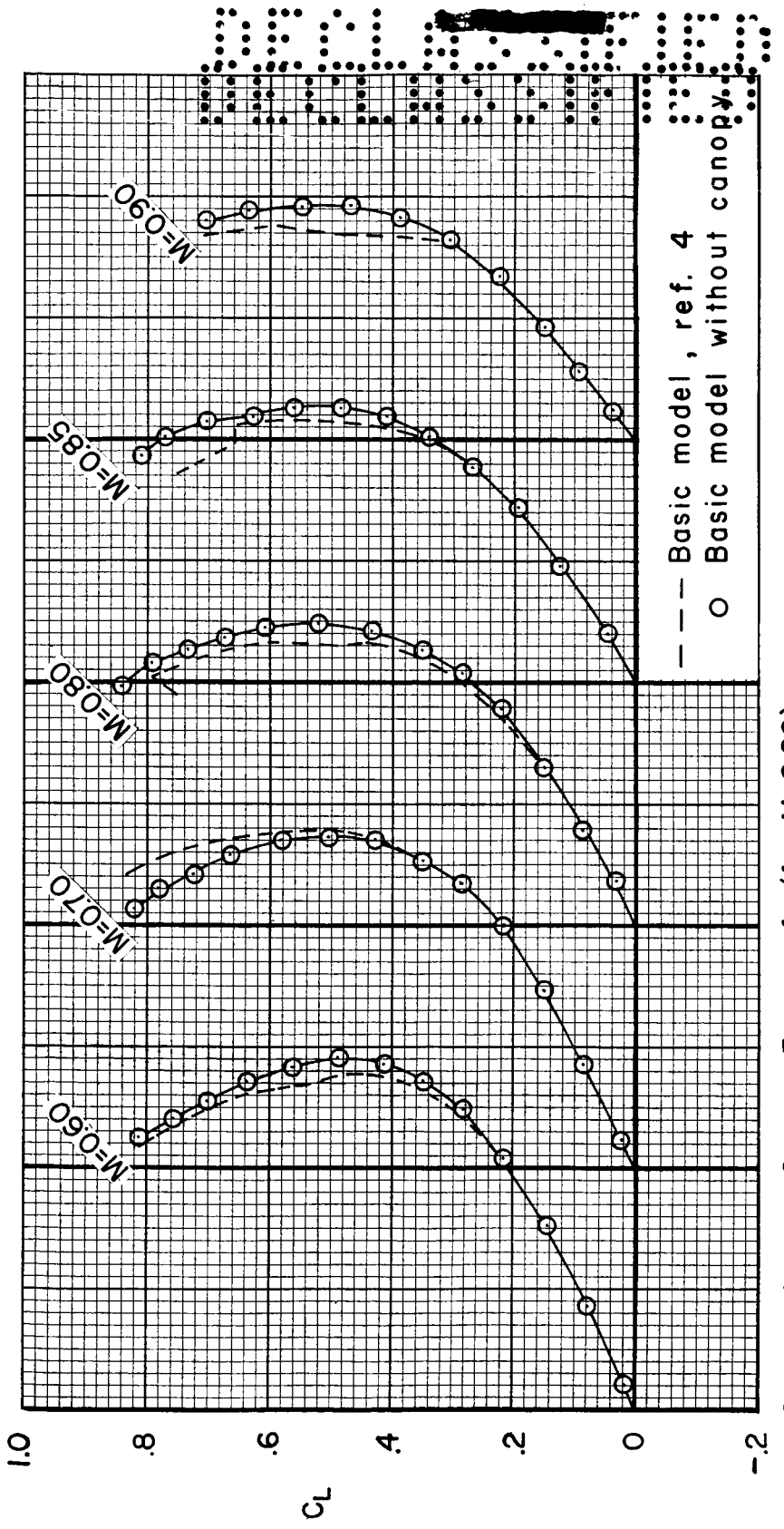

(c) Lift-drag ratio.

Figure 20.- Concluded.